

Ten dimensional symmetry of $\mathcal{N} = 4$ SYM correlators

Simon Caron-Huot, Frank Coronado

Department of Physics, McGill University, 3600 Rue University, Montréal, QC Canada H3A 2T8

E-mail: schuot@physics.mcgill.ca, fcidrogo@gmail.com

ABSTRACT: We consider four-point correlation functions of protected single-trace scalar operators in planar $\mathcal{N} = 4$ supersymmetric Yang-Mills (SYM). We conjecture that all loop corrections derive from an integrand which enjoys a ten-dimensional symmetry. This symmetry combines spacetime and R-charge transformations. By considering a 10D light-like limit, we extend the correlator/amplitude duality by equating large R-charge octagons with Coulomb branch scattering amplitudes. Using results from integrability, this predicts new finite amplitudes as well as some Feynman integrals.

Contents

1	Introduction	1
2	A review of correlators and loop integrands	3
2.1	Correlators and integrands	3
2.2	The stress tensor multiplet	5
2.3	Higher BPS operators and saturation	6
3	Ten-dimensional hidden symmetry	7
3.1	All free three-point and four-point functions	8
3.2	Hidden symmetry at one-loop	11
3.3	Conjectured 10-dimensional symmetry for higher-loop integrands	12
3.4	Two and three-loop correlators	13
3.5	Absence of Gram determinant ambiguities with 7 loops or less	14
4	Octagons as scattering amplitudes on the Coulomb branch	15
4.1	Example amplitudes on the restricted Coulomb branch	18
4.2	Comments on the four-dimensional massless limit	20
5	A Coulomb branch amplitude from integrability	22
5.1	Hexagonalization and octagons	22
5.2	The octagon from integrability: 10D null limit and weak coupling expansion	25
5.2.1	Octagon at weak coupling	26
5.3	Integrals from octagons	27
5.3.1	Detailed comparison at four-loops	29
5.3.2	Beyond the Basso-Dixon fishnets	31
6	Discussion	33
A	Definition of 3-loop conformal integrals	35
B	A five-loop identity	36

1 Introduction

The loop integrands of (some) correlation functions in planar $\mathcal{N} = 4$ SYM have hidden symmetries that highly constrain their form. The most interesting and studied example is the four-point correlator of scalars in the stress tensor multiplet. Because loop corrections

can be obtained by inserting the Lagrangian density, which is part of the same multiplet, the loop integrand enjoys a full permutation symmetry which treats the four external points and loop integration points on the same footing. This powerful symmetry has played a key role in “bootstrapping” the integrand [1, 2] (now up to ten loops [3]) by imposing various limits on an Ansatz of conformal integrals.

The stress tensor multiplet is the first of an infinite tower of protected (half-BPS) single-trace operators present in this theory. These have scaling dimension $\Delta = k$ with $k \geq 2$ and can be interpreted, in the $\text{AdS}_5 \times \text{S}_5$ dual realization of this theory, as Kaluza-Klein modes of the graviton on the five-sphere. They thus offer a unique window into the 10-dimensional nature of the dual theory. The combinatorics of their correlators $\mathcal{G}_{k_1 k_2 k_3 k_4}$ however becomes rapidly complicated because of the proliferation of R-charge structures. Furthermore, the full permutation symmetry that interchanges external and internal points is lost: the bootstrap problem has many more free parameters to fix. Nevertheless, with the discovery of a recursive relation between different integrands in their light-cone limit, all integrands were obtained up to three loops [4] and later to five loops using further input from integrability [5]. These results showed that each integrand $\mathcal{G}_{k_1 k_2 k_3 k_4}$ contains only a subgroup of the basis of conformal integrals from the stress tensor case \mathcal{G}_{2222} and, not surprisingly, this subset gets smaller as the charges k_i increase.

In this paper we propose that the integrands $\mathcal{G}_{k_1 k_2 k_3 k_4}$ all follow from a single generating function which enjoys a ten-dimensional hidden symmetry. At “low” loop orders (up to at least seven loops), this generating function can be uniquely uplifted from the known stress-tensor case by replacing all four-dimensional distances x_{ij}^2 by ten-dimensional ones $X_{ij}^2 \equiv x_{ij}^2 + y_{ij}^2$, where the y_i are null 6-vectors parametrizing the R-charge of the external operators. By expanding at small y_{ij}^2 and selecting terms with the correct charge, we have verified that this generating function reproduces precisely all $\mathcal{G}_{k_1 k_2 k_3 k_4}$ in the literature.

As an application, we observe that the ten-dimensional symmetry equates two natural limits in which correlators simplify or factorize: when an edge becomes “fat” from carrying a large R-charge, which prevents propagators from crossing it (at finite loop order), or when an edge becomes null, creating a high-energy excitation that can’t be deflected. Both are realized simply by taking the 10-dimensional null limit $X_{ij}^2 \rightarrow 0$. Combining this observation with the known relation between null limits and scattering amplitudes, we conjecture a new relation between scattering amplitudes on the Coulomb branch and the 10D null limit of charged correlators.

This conjecture implies that the so-called *octagon*, a family of four-point functions with large R-charge [6, 7], has the same integrand as the four-gluon amplitude. When restricted to a suitable subset of the Coulomb branch, on which infrared divergences of the amplitudes cancel, the integrated expressions also coincide. In other words, the octagon is a scattering amplitude. Exact results from integrability [8, 9] then allow to predict new integrated expressions for various (combinations of) Feynman integrals.

This paper is organized as follows. In section 2 we review known results on the loop integrands of half-BPS correlators, defined through the Lagrangian insertion method. In

section 3 we propose generating functions which unite them, first for free correlators and then for loop integrands. We make explicit the ten-dimensional symmetry of these generating functions and show that they uniquely uplift from the stress tensor case up to at least seven loops. In section 4 we consider a ten-dimensional null limit which allows us to establish a novel duality between correlators with large R-charge (octagons) and massive scattering amplitudes on the Coulomb branch. We argue this duality holds for their integrands and also at the integrated function level. We observe that different ways to approach the four-dimensional massless limit are controlled by exponents which differ from the cusp anomalous dimension. In section 5 we use recent integrability results to provide a finite coupling representation for the octagon/amplitude. We focus on the weak coupling limit where we can compare with scattering amplitude integrals. This allows us to rediscover the map between regular fishnet diagrams and determinants of ladder integrals, as well as extending it to include deformations of the fishnets. In section 6 we discuss our results and possible extensions. In appendix A we record a basis of three-loop planar integrals used in the main text. Finally, in appendix B, we exemplify a five-loop identity derived as a consequence of the duality.

2 A review of correlators and loop integrands

We consider $\mathcal{N} = 4$ super Yang-Mills with gauge group $SU(N_c)$ (or $U(N_c)$). In its gauge theory formulation, the theory contains six scalar fields $\Phi = (\phi^1, \dots, \phi^6)$ which are all $N_c \times N_c$ Hermitian matrices (traceless in the $SU(N_c)$ case). We will be interested in single-trace half-BPS protected operators, which are symmetric traceless (with respect to $SO(6)$) products of these scalars:

$$\mathcal{O}_{k_i}(x_i) = \frac{1}{k_i} \left(\frac{2}{4\pi^2 N_c} \right)^{k_i/2} \text{Tr}[(y_i \cdot \Phi(x_i))^{k_i}] \quad (2.1)$$

where we introduced null 6-vectors $y_i \cdot y_i = 0$ in order to automatically project out the traces. The chosen normalization, including $1/k$ which accounts for the cyclic symmetry of the trace in \mathcal{O}_k , will simplify future formulas. The operator $\mathcal{O}_{k_i}(x_i)$ is the lowest-dimensional component of a supermultiplet which also contains fermions, which will not be considered in this paper. To fix our notations, the two-point function in the planar limit is

$$\langle \mathcal{O}_k(x_1) \mathcal{O}_k(x_2) \rangle = \left(\frac{1}{k} + O(1/N_c^2) \right) (d_{12})^k \quad \text{where} \quad d_{ij} \equiv \frac{2 y_i \cdot y_j}{x_{ij}^2} = \frac{-y_{ij}^2}{x_{ij}^2} \quad (2.2)$$

with $x_{ij} = x_i - x_j$.¹

2.1 Correlators and integrands

The perturbative series of the connected planar four-point function takes the generic form:

$$N_c^2 \langle \mathcal{O}_{k_1} \mathcal{O}_{k_2} \mathcal{O}_{k_3} \mathcal{O}_{k_4} \rangle_c = G_{k_1 k_2 k_3 k_4}^{\text{free}} + \sum_{\ell=1}^{\infty} G_{k_1 k_2 k_3 k_4}^{(\ell)} + O(1/N_c^2), \quad (2.3)$$

¹In the literature, y_{ij}^2 is sometimes defined as a dot product: $(y_{ij}^2)^{\text{elsewhere}} = y_i \cdot y_j$. Here it will be advantageous to treat x (spacetime) and y (R-charge) variables symmetrically: $(y_{ij}^2)^{\text{here}} \equiv (y_i - y_j)^2$.

where the loop corrections can be computed using the Lagrangian insertion method [1, 10]:

$$G_{k_1 k_2 k_3 k_4}^{(\ell)} = \frac{(-g^2)^\ell}{\ell!} \int \frac{d^4 x_5}{\pi^2} \cdots \frac{d^4 x_{4+n}}{\pi^2} \mathcal{G}_{k_1 k_2 k_3 k_4}^{(\ell)}, \quad (2.4)$$

with $g^2 \equiv \frac{g_{YM}^2 N_c}{16\pi^2}$ the coupling constant. All our integrals are written after Wick rotation to Euclidean signature. The ℓ -loop integrand \mathcal{G} is given by a $(4 + \ell)$ -point correlator of the four external operators and ℓ Lagrangian densities evaluated at Born level

$$\mathcal{G}_{k_1 k_2 k_3 k_4}^{(\ell)} = \langle \mathcal{O}_{k_1} \mathcal{O}_{k_2} \mathcal{O}_{k_3} \mathcal{O}_{k_4} \mathcal{L}(x_5) \cdots \mathcal{L}(x_{4+\ell}) \rangle^{(0)}. \quad (2.5)$$

The superscript indicates that the correlator itself is computed only in the Born-level approximation which starts at order g^0 .

A partial non-renormalisation theorem imposes a factorization for the four-point correlator and its integrand [11]:

$$\mathcal{G}_{k_1 k_2 k_3 k_4}^{(\ell)} = R_{1234} (2 x_{12}^2 x_{13}^2 x_{14}^2 x_{23}^2 x_{24}^2 x_{34}^2) \mathcal{H}_{k_1 k_2 k_3 k_4}^{(\ell)}. \quad (2.6)$$

The first factor has conformal weight (-1) and harmonic weight 2 at each point:

$$R_{1234} = d_{13}^2 d_{24}^2 x_{13}^2 x_{24}^2 + d_{12} d_{23} d_{34} d_{14} (x_{13}^2 x_{24}^2 - x_{12}^2 x_{34}^2 - x_{14}^2 x_{23}^2) + (1 \leftrightarrow 2) + (1 \leftrightarrow 4). \quad (2.7)$$

The reduced integrand \mathcal{H} then transforms like a correlator of operators of charge $(k_i - 2)$ and dimensions $(k_i + 2)$. In particular, the reduced stress-tensor correlator \mathcal{H}_{2222} is independent of y variables.

In the literature, a generic \mathcal{H} is typically expanded as a sum of various R-charge structures distinguished by the exponents of d_{ij} :

$$\mathcal{H}_{k_1 k_2 k_3 k_4}^{(\ell)} = \sum_{\substack{\{b_{ij}\} \\ k_i = 2 + \sum_j b_{ij}}} \mathcal{F}_{\{b_{ij}\}}^{(\ell)} \times \prod_{1 \leq i < j \leq 4} (d_{ij})^{b_{ij}} \quad (2.8)$$

where the six-tuples $\{b_{ij}\} \equiv \{b_{12}, b_{13}, b_{14}, b_{23}, b_{24}, b_{34}\}$ satisfy the constraints $k_i = 2 + \sum_{j \neq i} b_{ij}$.

This can be interpreted as listing every possible tree-level R-symmetry structure (products of d_{ij} 's) and dressing them with loop corrections. Importantly, the integrands $\mathcal{F}_{\{b_{ij}\}}$ are rational functions. They depend exclusively on x_{ij}^2 and have the following three defining properties:

- \mathcal{F} has conformal weight 4 at each point.
- $\mathcal{F}^{(\ell)}$ has an S_ℓ symmetry on the integration points $x_5, \dots, x_{\ell+4}$.
- As a consequence of a OPE analysis, \mathcal{F} contains at most a single pole in each x_{ij}^2 .

These properties allow one to make an ansatz for \mathcal{F} with a finite number of parameters. At one loop, for example, these conditions are restrictive enough to fix all these structures to be given by the same simple product:

$$\mathcal{F}_{\{b_{ij}\}}^{(1)} = \frac{1}{\prod_{1 \leq i < j \leq 5} x_{ij}^2} \quad \text{for all } b_{ij} \geq 0. \quad (2.9)$$

The fact that the proportionality constant is the same for all R-charges follows from simple factorization limits which will be reviewed below. At higher loops, more conditions, coming for example from Euclidean or Lorentzian OPEs, are required to uniquely bootstrap the integrands. In what follows we review the results on the integrand of stress tensor multiplets, which has been pushed up to ten loops, and we review analogous results for charged correlators.

2.2 The stress tensor multiplet

The case $k_i = 2$ is special since as noted the reduced integrand \mathcal{H}_{2222} is independent of y_{ij}^2 and thus consists of a single structure at each loop order (see eq. (2.8)):

$$\mathcal{H}_{2222}^{(\ell)} = \mathcal{F}_{\{0,0,0,0,0\}}^{(\ell)}. \quad (2.10)$$

In addition, apart from the obvious permutation symmetries $S_4 \times S_n$ which permute the external and internal points separately, this object enjoys a remarkable full permutation symmetry S_{4+n} which interchanges external and internal points [1]. This special symmetry stems from the fact that \mathcal{O}_2 and the Lagrangian density \mathcal{L} are parts of the same supermultiplet, being respectively its bottom and top ($\sim \theta^4$) components.

Up to three loops, the extended permutation symmetry and planarity are strong enough to fix the integrands up to an overall constant [2]:

$$\mathcal{H}_{2222}^{(1)} = \frac{1}{\prod_{1 \leq i < j \leq 5} x_{ij}^2}, \quad (2.11)$$

$$\mathcal{H}_{2222}^{(2)} = \frac{1}{48} \frac{x_{12}^2 x_{34}^2 x_{56}^2 + S_6 \text{ permutations}}{\prod_{1 \leq i < j \leq 6} x_{ij}^2}, \quad (2.12)$$

$$\mathcal{H}_{2222}^{(3)} = \frac{1}{20} \frac{(x_{12}^2)^2 (x_{34}^2 x_{45}^2 x_{56}^2 x_{67}^2 x_{73}^2) + S_7 \text{ permutations}}{\prod_{1 \leq i < j \leq 7} x_{ij}^2}. \quad (2.13)$$

Notice that each of these is seeded by a single monomial by summing over S_{4+n} permutations of all points x_1, \dots, x_{4+n} . The shown denominators simply remove equivalent permutations, e.g. the two-loop integrand in (2.12) consists of 15 distinct terms with unit coefficient.

These integrands determine, through eqs. (2.4) and (2.6), the two-loop correlator:

$$G_{2222}^{(1)} = -2 g^2 R_{1234} \times g_{1234}, \quad (2.14)$$

$$G_{2222}^{(2)} = 2 g^4 R_{1234} \left(h_{12;34} + h_{34;12} + h_{14;23} + h_{23;14} + h_{13;24} + h_{24;13} + \frac{1}{2} (x_{12}^2 x_{34}^2 + x_{13}^2 x_{24}^2 + x_{14}^2 x_{23}^2) [g_{1234}]^2 \right), \quad (2.15)$$

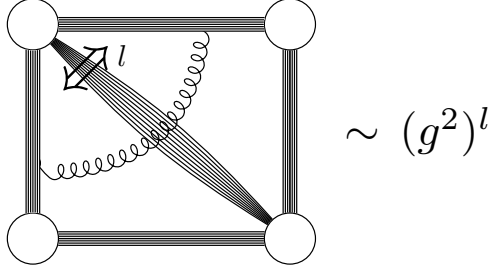


Figure 1: Saturation: an R-charge factor $(d_{ij})^l$ requires a “bridge” made of l propagators and cannot be crossed without paying a factor $(g^2)^l$.

in terms of one-loop and two-loop ladder integrals:

$$\begin{aligned}
 g_{1234} &= \frac{1}{\pi^2} \int \frac{d^4 x_5}{x_{15}^2 x_{25}^2 x_{35}^2 x_{45}^2} = \frac{F_1(z, \bar{z})}{x_{13}^2 x_{24}^2}, \\
 h_{13;24} &= \frac{x_{24}^2}{\pi^4} \int \frac{d^4 x_5 d^4 x_6}{(x_{15}^2 x_{25}^2 x_{45}^2) x_{56}^2 (x_{26}^2 x_{36}^2 x_{46}^2)} = \frac{F_2(z, \bar{z})}{x_{13}^2 x_{24}^2}.
 \end{aligned} \tag{2.16}$$

The function F is recorded in eq. (5.12) below and the cross-ratios satisfy:

$$z\bar{z} = \frac{x_{12}^2 x_{34}^2}{x_{13}^2 x_{24}^2}, \quad (1-z)(1-\bar{z}) = \frac{x_{23}^2 x_{14}^2}{x_{13}^2 x_{24}^2}. \tag{2.17}$$

Similarly, R-charge cross ratios $\alpha, \bar{\alpha}$ are defined using y_{ij}^2 .

At four and higher loops, the basis of homogeneous polynomials grows as: 3, 7, 36, 220, \dots . In order to fix the coefficients of these polynomials in an Ansatz, one needs more conditions on the integrand or integrated correlator. This was achieved by the analysis of kinematical limits which are constrained by factorization, what is called the soft-collinear bootstrap [12, 13]. As a simple illustration, if $\{x_{12}^2, x_{23}^2, x_{34}^2, x_{41}^2\} \rightarrow 0$ describes a null square, then in the limit that x_5 approaches an edge, the most singular term factorizes: $\mathcal{H}^{(\ell)} \rightarrow (\frac{2x_{13}^2 x_{24}^2}{x_{15}^2 x_{25}^2 x_{35}^2 x_{45}^2}) \times \mathcal{H}^{(\ell-1)}$. Physically, this ensures the exponentiation of collinear divergences of a dual scattering amplitude. These lead to linear equations that must be satisfied by the coefficients in the Ansatz. Such relations and generalizations allowed to completely fix the planar integrand now up to 10 loops [2, 3, 13].

2.3 Higher BPS operators and saturation

Moving to charged correlators, the number of structures $\mathcal{F}_{\{b_{ij}\}}$ to determine would appear to be infinite, however the number of distinct functions at a given loop order is finite. This is due to a saturation bound: if a propagator becomes too “fat” it cannot be crossed, as depicted below in fig. 1. Adding more propagators will not change the result, leading to

$$\mathcal{F}_{\{b_{12}, \dots\}}^{(\ell)} \equiv \mathcal{F}_{\{\kappa_n, \dots\}}^{(\ell)} \quad \text{if } b_{12} \geq \kappa_n. \tag{2.18}$$

$\{b_{ij}\}$	$\begin{array}{c} 1 \text{ } \overline{\text{---}} \text{ } 2 \\ 4 \text{ } \text{---} \text{ } 3 \end{array}$	c_{gg}^1	c_{gg}^2	c_{gg}^3	c_h^1	c_h^2	c_h^3
$\{0, 0, 0, 0, 0, 0, 0\}$	$\begin{array}{c} \cdot \\ \cdot \\ \cdot \end{array}$	1	1	1	2	2	2
$\{\beta_1, 0, 0, 0, 0, 0, 0\}$	$\begin{array}{c} \text{---} \\ \cdot \\ \cdot \end{array}$	0	1	1	1	2	2
$\{\beta_1, \beta_2, 0, 0, 0, 0, 0\}$	$\begin{array}{c} \text{---} \\ \cdot \\ \cdot \end{array}$	0	0	1	1	1	2
$\{\beta_1, \beta_2, 0, \beta_3, 0, 0, 0\}$ $\{\beta_1, \beta_2, \beta_3, 0, 0, 0, 0\}$	$\begin{array}{c} \cdot \\ \cdot \\ \cdot \end{array}$	0	0	0	1	1	1
$\{0, 0, \beta_1, \beta_2, 0, 0, 0\}$	$\begin{array}{c} \text{---} \\ \text{---} \\ \cdot \end{array}$	1	1	0	2	2	0
$\{\beta_1, 0, \beta_2, \beta_3, 0, 0, 0\}$	$\begin{array}{c} \text{---} \\ \text{---} \\ \cdot \end{array}$	0	1	0	1	2	0
$\{\beta_1, \beta_2, \beta_3, \beta_4, 0, 0, 0\}$	$\begin{array}{c} \text{---} \\ \text{---} \\ \cdot \end{array}$	0	0	0	1	1	0
$\{0, \beta_1, \beta_2, \beta_3, \beta_4, 0, 0\}$	$\begin{array}{c} \text{---} \\ \text{---} \\ \cdot \end{array}$	1	0	0	2	0	0
$\{\beta_1, \beta_2, \beta_3, \beta_4, \beta_5, 0, 0\}$	$\begin{array}{c} \text{---} \\ \text{---} \\ \cdot \end{array}$	0	0	0	1	0	0
$\{\beta_1, \beta_2, \beta_3, \beta_4, \beta_5, \beta_6\}$	$\begin{array}{c} \text{---} \\ \text{---} \\ \cdot \end{array}$	0	0	0	0	0	0

Figure 2: The full set of two-loop integrands $\mathcal{F}_{b_{ij}}$ according to [4], showing only inequivalent R -charge structures. The coefficients enter eq. (2.20). All values $\beta_i \geq 1$ are equivalent due to the saturation phenomenon.

Up to five loops saturation happens at $\kappa_n = n - 1$, according to [4, 5], however this can change at higher loop orders. Another useful fact is that singularities from propagator poles are also “uncrossable”, meaning that residues saturate already at $b_{12} = 0$:

$$\text{Res}_{x_{12}^2=0} \mathcal{F}_{\{b_{ij}\}} = \text{Res}_{x_{12}^2=0} \mathcal{F}_{\{b_{ij}\}} \Big|_{b_{12} \rightarrow 0}. \quad (2.19)$$

These two conditions will be important below. As discussed in ref. [4], they explain much of the structure of R -charged integrands. As an example we display here the two-loop results for the integrated structures $\mathcal{F}_{\{b_{ij}\}}$ from that reference, in terms of the integrals entering in (2.14) and with coefficients recorded in fig. 2:

$$x_{12}^2 x_{13}^2 x_{14}^2 x_{23}^2 x_{24}^2 x_{34}^2 \int \frac{dx_5^4 dx_6^4}{2!(\pi^2)^2} \mathcal{F}_{\{b_{ij}\}}^{(2)} = c_h^1 h_{12;34} + c_h^2 h_{13;24} + c_h^3 h_{14;23} + \frac{1}{2} (c_{gg}^1 x_{12}^2 x_{34}^2 + c_{gg}^2 x_{13}^2 x_{24}^2 + c_{gg}^3 x_{14}^2 x_{23}^2) [g_{1234}]^2. \quad (2.20)$$

In the next section, we explain how to fully recover the information in such tables from a concise ten-dimensional integrand.

3 Ten-dimensional hidden symmetry

Our goal is now to understand how different R -charge correlators fit together as a single object. The key idea will be to define a “master” operator given as a sum of all scalar BPS

operators:

$$\mathcal{O}(x, y) \equiv \sum_{k=1}^{\infty} \mathcal{O}_k(x, y). \quad (3.1)$$

The operator \mathcal{O}_1 vanishes when we consider $SU(N_c)$ gauge group, in which case the sum starts effectively from \mathcal{O}_2 . For the free correlators it will be more convenient to work in the $U(N_c)$; formulas for $SU(N_c)$ are then trivially obtained by subtracting off terms linear in y . For the loop integrands, there will be no differences between $U(N_c)$ and $SU(N_c)$.

To create a generating function of R-charged correlators, we simply evaluate correlation functions of these master operators:

$$\langle \mathcal{O}(x_1, y_1) \mathcal{O}(x_2, y_2) \cdots \rangle. \quad (3.2)$$

As a warm-up, we first perform this task for the free theory, starting with three- and four-point functions. After stating our main conjecture in subsection 3.3, we discuss loop integrands as well as integrated correlators in 3.4.

3.1 All free three-point and four-point functions

The three-point functions of our BPS operators are protected so the free theory result is exact and it is given by a single R-charge structure [14]:

$$\langle \mathcal{O}_{k_1} \mathcal{O}_{k_2} \mathcal{O}_{k_3} \rangle = \frac{1}{N_c} (d_{12})^{l_{12}} (d_{23})^{l_{23}} (d_{31})^{l_{31}} \quad (3.3)$$

with $l_{12} = \frac{k_1+k_2-k_3}{2} \geq 0$ and cyclic rotations of this for l_{23} and l_{31} . Our normalization in (2.1), with $1/k$ for each \mathcal{O}_k , conveniently cancels the cyclic permutations of each operator. This was chosen so that the three-point functions will sum up to a geometric series.

The generating function of all three-point functions is computed as

$$\langle \mathcal{O}(x_1, y_1) \mathcal{O}(x_2, y_2) \mathcal{O}(x_3, y_3) \rangle = \sum_{l_{ij} \geq 1} \langle \mathcal{O}_{k_1} \mathcal{O}_{k_2} \mathcal{O}_{k_3} \rangle + \frac{1}{N_c} \mathbb{T}_{\text{extr}} \quad (3.4)$$

where we separated generic terms from those with zero-length bridge, often called “extremal” correlators, see fig. 3. Introducing a new effective propagator:

$$D_{ij} \equiv \frac{d_{ij}}{1-d_{ij}} = \frac{-y_{ij}^2}{X_{ij}^2} \quad (3.5)$$

which involves the ten-dimensional distance that combines spacetime and R-charge space,

$$X_{ij}^2 \equiv x_{ij}^2 + y_{ij}^2, \quad (3.6)$$

the correlator becomes simply

$$\langle \mathcal{O}(x_1, y_1) \mathcal{O}(x_2, y_2) \mathcal{O}(x_3, y_3) \rangle = \frac{1}{N_c} D_{12} D_{23} D_{31} + \frac{1}{N_c} \mathbb{T}_{\text{extr}}. \quad (3.7)$$

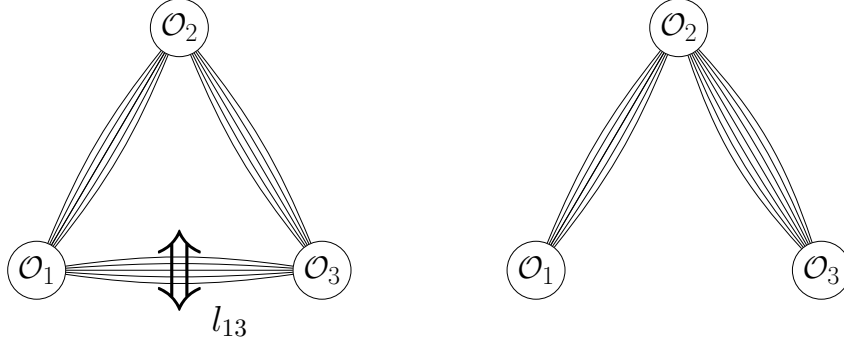


Figure 3: Generic versus extremal three-point functions. The second type can be removed by redefining \mathcal{O} 's to be orthogonal to double-trace operators.

In order to unpack the correlators from the generating function, one can simply expand back the geometric series:

$$\frac{d_{ij}}{1 - d_{ij}} = \sum_{a=1}^{\infty} (d_{ij})^a \quad (3.8)$$

and read-off the individual correlators according to their R-charge (exponents of d_{ij}).

The second term \mathbb{T}_{extr} in the generating function (3.4) represents the contribution of the extremal three-point functions with topology shown in figure. Unlike the fully connected part, the extremal part differs slightly for $U(N_c)$ and $SU(N_c)$:

$$\mathbb{T}_{extr}^{U(N_c)} = D_{12}D_{23} + D_{23}D_{31} + D_{31}D_{12}, \quad (3.9)$$

$$\mathbb{T}_{extr}^{SU(N_c)} = d_{12}d_{23}D_{12}D_{23} + d_{23}d_{31}D_{23}D_{31} + d_{31}d_{12}D_{31}D_{12}. \quad (3.10)$$

The role of the extra factors d_{ij} in the $SU(N_c)$ case is to shift the lowest R-charge from \mathcal{O}_1 to \mathcal{O}_2 . This result could in principle be written exclusively in terms of our effective propagator using: $d_{ij} = \frac{D_{ij}}{1+D_{ij}}$, at the cost of breaking the polynomial structure on D_{ij} .

In fact, there is a natural third option for \mathbb{T}_{extr} : it can be removed altogether by a change in operator basis. Indeed, order by order in $1/N_c$, it is often natural to add a multiple of multi-trace operators to single-trace ones, in order to make them mutually orthogonal. This is called the single-particle basis in refs. [15, 16]. In this basis, by definition, \mathbb{T}_{extr} vanishes:

$$\mathbb{T}_{extr}^{SP} = 0 \quad \text{where} \quad \mathcal{O}_k^{SP} \equiv \mathcal{O}_k + \sum_{k'} a_{k,k'} \mathcal{O}_{k'} \mathcal{O}_{k-k'} + \dots \quad (3.11)$$

Let us move on to four-point functions. In the free theory these can be similarly written as a sum over tree-level graphs labelled by six propagator powers l_{ij} where $1 \leq i < j \leq 4$. Some graphs occur with different symmetry factors; for example, the free correlator with

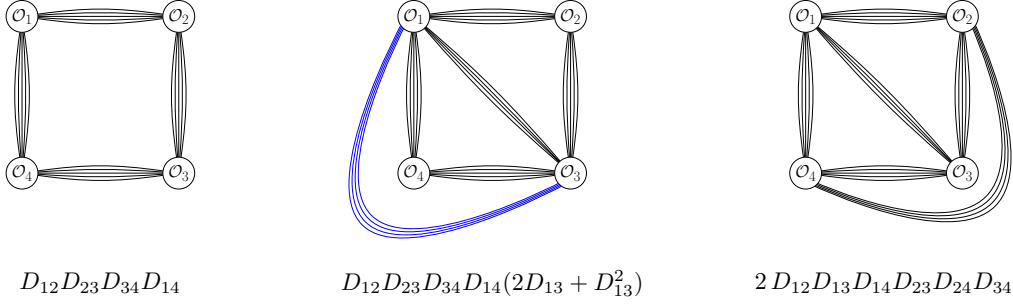


Figure 4: Non-extremal four-point topologies, where each operator couples to at least two distinct other operators. Bundles denote products of one or more Wick contractions.

equal weights is:

$$\begin{aligned}
G_{kkkk}^{\text{free}} &= \sum_{a=1}^{k-1} (d_{12}d_{34})^a (d_{23}d_{14})^{k-a} + (1 \leftrightarrow 2) + (1 \leftrightarrow 4) \\
&\quad + \sum_{a=2}^{k-1} \sum_{b=1}^{a-1} 2 (d_{12}d_{34})^{k-a} (d_{13}d_{24})^{a-b} (d_{14}d_{23})^b
\end{aligned} \tag{3.12}$$

where the operations such as $(1 \leftrightarrow 2)$ act on the first term by swapping the indexes of d_{ij} . Similar results are known for correlators with different weights, for example in [17] (appendix B.1 therein).

In principle, by summing such formulas, one could compute the generating function:

$$G^{\text{free}} \equiv N_c^2 \langle \mathcal{O}(x_1, y_1) \mathcal{O}(x_2, y_2) \mathcal{O}(x_3, y_3) \mathcal{O}(x_4, y_4) \rangle_c = \sum_{k_i \geq 1} G_{k_1 k_2 k_3 k_4}^{\text{free}}. \tag{3.13}$$

The easiest way however is to enumerate the possible topologies as shown in fig. 4. Since each graph in each family comes with the same symmetry factor up to a factor $k_1 k_2 k_3 k_4$ (coming from cyclic permutations of each operator) which cancels out in the definition of \mathcal{O}_k (see eq. (2.1)), each bundle simply yields the ten-dimensional propagator D_{ij} . Adding the topologies then gives the generating function of four-point correlators:

$$\begin{aligned}
G^{\text{free}} &= D_{12}D_{23}D_{34}D_{14}(1 + 2D_{13} + D_{13}^2 + 2D_{24} + D_{24}^2) + (1 \leftrightarrow 2) + (1 \leftrightarrow 4) \\
&\quad + 2D_{12}D_{13}D_{14}D_{23}D_{24}D_{34} + G_{\text{extr}}^{\text{free}}.
\end{aligned} \tag{3.14}$$

The first term, $D_{12}D_{13}D_{34}D_{14}$, generates all graphs with four bundles forming a square with corners (1234) and arbitrary number of propagators on each bundle, see figure 4. Furthermore, when dressed with the factor:

$$2D_{13} + D_{13}^2 = \sum_{a=1}^{\infty} (a+1) (d_{13})^a \tag{3.15}$$

it gives all graphs with extra propagators between operators \mathcal{O}_1 and \mathcal{O}_3 . The coefficient $a+1$ on the right-hand side gives the number of ways of splitting the diagonal bundle with a

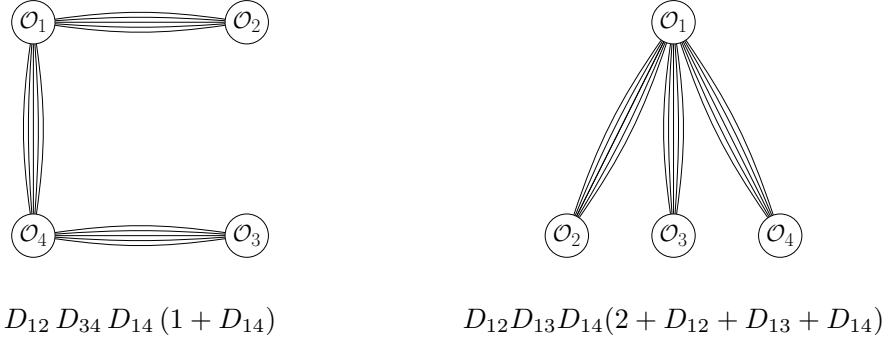


Figure 5: Extremal topologies. At the bottom the corresponding generating function for the $U(N_c)$ case.

propagators distributed between the inside and outside of the square frame as shown in the figure.

Other terms in (3.14) give permutations of the square frame and its diagonals. The last term generates all graphs with all six bundles turned on between the six distinct pairs, see figure. The factor of 2 accounts for the two distinct ways of drawing the diagonals inside or outside the square frame.

Diagrams contributing to the extremal pieces are shown in fig. 5. As in the previous three-point example, the “extremal” piece vanishes in the single-particle basis:

$$G_{\text{extr}}^{\text{free}, SP} = 0. \quad (3.16)$$

We record for completeness the result in the field theory basis in the $U(N_c)$ case:

$$\begin{aligned} G_{\text{extr}}^{\text{free}, U(N_c)} &= D_{12} D_{34} D_{14} (1 + D_{14}) + (11 \text{ permutations}) \\ &\quad + D_{12} D_{34} D_{14} D_{13} (2 + D_{14} + D_{13}) + (11 \text{ permutations}) \\ &\quad + D_{12} D_{13} D_{14} (2 + D_{12} + D_{13} + D_{14}) + (3 \text{ permutations}). \end{aligned} \quad (3.17)$$

This generates all graphs which become disconnected after removing one bundle. For instance, the first and third lines in (3.17) generate the topologies in figure 5. The $SU(N_c)$ result can be obtained straightforwardly from this by subtracting terms with only a single power of any given d_{ij} . For the first two lines, this amounts to simple multiplication with extra d_{ij} factors, but for the third line the result is much less elegant.

At loop level, $U(1)$ factors and extremal structures decouple, because the $U(1)$ sector is non-interacting and extremal structures would represent loop corrections to 3- or 2- point functions, which are protected. Therefore, for loop corrections, we will not need to distinguish SP , $U(N_c)$ or $SU(N_c)$ correlators.

3.2 Hidden symmetry at one-loop

We saw that geometric series of free theory correlators are concisely captured by using ten-dimensional propagators $D_{ij} = \frac{y_{ij}^2}{X_{ij}^2}$. Yet, free correlators do not enjoy ten-dimensional sym-

metry because of the y_{ij}^2 numerators in D_{ij} . However, we will find that loop integrands, for the *reduced* correlators, *do* enjoy a full 10D symmetry!

At one loop, the integrand was recorded in eq. (2.9), which we repeat for convenience:

$$\mathcal{H}_{k_1 k_2 k_3 k_4}^{(1)} = \frac{1}{\prod_{1 \leq i < j \leq 5} x_{ij}^2} \sum_{\substack{\{b_{ij}\} \\ k_i = 2 + \sum_j b_{ij}}} \times \prod_{1 \leq i < j \leq 4} (d_{ij})^{b_{ij}}. \quad (3.18)$$

Summing over k_i one finds independent geometric series in each b_{ij} . Recalling that $d_{ij} = \frac{-y_{ij}^2}{x_{ij}^2}$, this can be written entirely in terms of ten-dimensional distances!

$$\mathcal{H}^{(1)}(X_{ij}^2) = \frac{1}{\prod_{1 \leq i < j \leq 5} X_{ij}^2} \quad \text{with} \quad X_{ij}^2 = x_{ij}^2 + y_{ij}^2. \quad (3.19)$$

For $i \geq 5$ we set $y_i = 0$. We stress that ten-dimensional symmetry holds for the *reduced* correlator \mathcal{H} but not for \mathcal{G} itself.

The planarity of the one-loop correction (3.19) deserves comment—the displayed product does not correspond to a planar graph! However, analyzing the factor R_{1234} from eq. (2.7), one finds that it can be written as a sum of terms which each contain at least one X_{ij}^2 factor. This suffices to make the product $R_{1234}\mathcal{H}^{(1)}$ planar. A similar phenomenon was noticed in the integrability context [18]. At higher loops, $\mathcal{H}^{(\ell)}$ itself will be a sum of planar integrands.

In this example, the 10-dimensional symmetry could be turned around to recover the generic correlator from the simplest case:

$$\mathcal{H}^{(1)}(x, y) = \mathcal{H}_{2222}^{(1)}(x) \Big|_{x_{ij}^2 \rightarrow x_{ij}^2 + y_{ij}^2}. \quad (3.20)$$

This is a powerful observation which will be put to use in the next subsections.

3.3 Conjectured 10-dimensional symmetry for higher-loop integrands

We are ready to state our main conjecture: that the (reduced) integrands at each loop order derive from a generating function $\mathcal{H}^{(\ell)}(X_{ij}^2)$ which enjoys full ten-dimensional conformal symmetry, and full permutation symmetry in $\ell + 4$ coordinates.

A given correlator is obtained simply by extracting the coefficient of the correct power of y_i , explicitly:

$$\boxed{\mathcal{H}_{k_1 k_2 k_3 k_4}^{(\ell)}(x_{ij}^2, y_{ij}^2) = \text{coefficient of } \left(\prod_{i=1}^4 \beta_i^{k_i - 2} \right) \text{ in } \mathcal{H}^{(\ell)}(X_{ij}^2) \Big|_{y_{ij}^2 \rightarrow \beta_i \beta_j y_{ij}^2}}, \quad (3.21)$$

where we recall that $X_{ij}^2 = x_{ij}^2 + y_{ij}^2$. The same dictionary was introduced previously in the supergravity limit [17].

In particular this implies that the truncation from 10D to 4D of the generating function is the integrand of the simplest multiplet:

$$\lim_{X_{ij}^2 \rightarrow x_{ij}^2} \mathcal{H}^{(\ell)}(X_{ij}^2) = \mathcal{H}_{2222}(x_{ij}^2). \quad (3.22)$$

Conversely, the conjecture implies that the $\mathcal{H}_{2222}^{(\ell)}$ integrand determines all other correlators modulo functions which vanish in $D = 4$, that is, vanishing Gram determinants:

$$\mathcal{H}^{(\ell)}(X_{ij}^2) = \mathcal{H}_{2222}^{(\ell)}(x_{ij}^2) \Big|_{x_{ij}^2 \mapsto X_{ij}^2} + (\text{Gram determinants}). \quad (3.23)$$

As will be discussed in section 3.5, no planar, permutation symmetric, conformally invariant Gram determinant identity exist below 8 loops. Equations (3.21) and (3.23) thus unambiguously predicts all R-charged correlators up to at least 7-loops.

3.4 Two and three-loop correlators

Let us illustrate the preceding conjecture at low loop orders. The two-loop generating function obtained from (2.12) using the replacement (3.23) is simply:

$$\mathcal{H}^{(2)} = \frac{X_{12}^2 X_{34}^2 X_{56}^2 + 14 \text{ permutations}}{\prod_{1 \leq i < j \leq 6} X_{ij}^2}. \quad (3.24)$$

To relate this to usual correlators, different permutations of the 6 coordinates will be treated differently. We recall that $y_i = 0$ for the Lagrangian insertions ($i \geq 5$), so that for example $X_{i5}^2 = x_{i5}^2$. For the other distances we use the relation $X_{ij}^2 = (1 - d_{ij})x_{ij}^2$:

$$\mathcal{H}^{(2)} = \frac{1}{\prod_{1 \leq i < j \leq 4} (1 - d_{ij}) \prod_{1 \leq i < j \leq 6} x_{ij}^2} (1 + \sigma + \sigma^2) \quad (3.25)$$

$$\left((1 - d_{12})(1 - d_{34})x_{12}^2 x_{34}^2 x_{56}^2 + [(1 - d_{34})x_{34}^2 x_{16}^2 x_{25}^2 + (1 - d_{12})x_{12}^2 x_{45}^2 x_{36}^2 + (5 \leftrightarrow 6)] \right)$$

where σ denotes a cyclic rotation of (234). The correlators \mathcal{F} defined in eq. (2.8) may then be read off simply by expanding the geometric series $\frac{1}{1-d_{ij}} = \sum_{m=0}^{\infty} (d_{ij})^m$ and collecting all terms with common powers $(d_{ij})^{b_{ij}}$:

$$\mathcal{H}^{(\ell)} = \sum_{b_{ij} \geq 0} \mathcal{F}_{\{b_{ij}\}}^{(\ell)} \prod_{1 \leq i < j \leq 4} (d_{ij})^{b_{ij}}. \quad (3.26)$$

Some of the simplest are:

$$\mathcal{F}_{\{0,0,1,1,1,1\}}^{(2)} = \left(\frac{x_{13}^2}{(x_{15}^2 x_{25}^2 x_{35}^2) x_{56}^2 (x_{16}^2 x_{36}^2 x_{46}^2)} + (x_5 \leftrightarrow x_6) \right) + (x_2 \leftrightarrow x_3), \quad (3.27)$$

$$\mathcal{F}_{\{1,0,1,1,1,1\}}^{(2)} = \frac{x_{13}^2}{(x_{15}^2 x_{25}^2 x_{35}^2) x_{56}^2 (x_{16}^2 x_{36}^2 x_{46}^2)} + (x_5 \leftrightarrow x_6), \quad (3.28)$$

$$\mathcal{F}_{\{1,1,1,1,1,1\}}^{(2)} = 0. \quad (3.29)$$

and similarly $\mathcal{F}_{\{0,\beta_1,\beta_2,\beta_3,\beta_4,\beta_5\}}^{(2)} = \mathcal{F}_{\{0,1,1,1,1,1\}}^{(2)}$ when all $\beta_i \geq 1$. We see also that the one-loop-squared integral only appears in \mathcal{F} with two or more zeros, for instance:

$$\mathcal{F}_{\{1,0,1,1,0,1\}}^{(2)} = \frac{x_{13}^2 x_{24}^2}{\prod_{a=5,6} \prod_{i=1,2,3,4} x_{ia}^2} + \left[\frac{1}{(x_{15}^2 x_{25}^2) x_{56}^2 (x_{36}^2 x_{46}^2)} \left(\frac{x_{13}^2}{x_{35}^2 x_{16}^2} + \frac{x_{24}^2}{x_{45}^2 x_{26}^2} \right) + (x_5 \leftrightarrow x_6) \right]. \quad (3.30)$$

Moving to integrated expressions, since the d_{ij} factors commute with integration over $x_{i \geq 5}$, a generating function of R-charged correlators immediately follows:

$$G^{(\ell)} \equiv \sum_{k_i \geq 2} G_{k_1 k_2 k_3 k_4}^{(\ell)} = \frac{(-g^2)^\ell}{\ell!} R_{1234} (2 x_{12}^2 x_{13}^2 x_{14}^2 x_{23}^2 x_{24}^2 x_{34}^2) \int \frac{dx_5^4}{\pi^2} \dots \frac{dx_{4+n}^4}{\pi^2} \mathcal{H}^{(\ell)}. \quad (3.31)$$

At one and two-loops, the formulas recorded above give

$$G^{(1)} = -2g^2 R_{1234} g_{1234} \prod_{1 \leq i < j \leq 4} \frac{1}{1 - d_{ij}}, \quad (3.32)$$

$$G^{(2)} = 2g^4 R_{1234} \left(c_h^1 h_{12;34} + c_h^2 h_{13;24} + c_h^3 h_{14;23} + \frac{1}{2} (c_{gg}^1 x_{12}^2 x_{34}^2 + c_{gg}^2 x_{13}^2 x_{24}^2 + c_{gg}^3 x_{14}^2 x_{23}^2) [g_{1234}]^2 \right) \quad (3.33)$$

where g and h are the one- and two-loop ladders defined in eq. (2.16), and the independent coefficients are:

$$c_h^1 = \frac{(1 - d_{12}) + (1 - d_{34})}{\prod_{1 \leq i < j \leq 4} (1 - d_{ij})} \quad \text{and} \quad c_{gg}^1 = \frac{(1 - d_{12})(1 - d_{34})}{\prod_{1 \leq i < j \leq 4} (1 - d_{ij})}. \quad (3.34)$$

Through these manipulations, we have shown that eq. (3.24) fully reproduces table 2!

At three-loops, all R-charged correlators can now be obtained similarly by uplifting (2.13), which yields:

$$\begin{aligned} G^{(3)} = & -2g^6 R_{1234} \left(c_{gh}^1 (g \times h)_{12;34} + c_{gh}^2 (g \times h)_{13;24} + c_{gh}^3 (g \times h)_{14;23} \right. \\ & + c_L^1 L_{12;34} + c_L^2 L_{13;24} + c_L^3 L_{14;23} + c_E^1 E_{12;34} + c_E^2 E_{13;24} + c_E^3 E_{14;23} \\ & \left. + \frac{1}{2} (c_H^1 + c_H^2 1/v) H_{12;34} + \frac{1}{2} (c_H^3 + c_H^4 u/v) H_{13;24} + \frac{1}{2} (c_H^5 + c_H^6 u) H_{14;23} \right) \quad (3.35) \end{aligned}$$

with the conformal integrals given in appendix A and coefficients (with $P_4 \equiv \prod_{1 \leq i < j \leq 4} (1 - d_{ij})$):

$$\begin{aligned} c_{gh}^1 &= (1 - d_{12})(1 - d_{34})[(1 - d_{12}) + (1 - d_{34})]/P_4, \\ c_L^1 &= [(1 - d_{12})^2 + (1 - d_{34})^2 + 2(1 - d_{12}) + 2(1 - d_{34})]/P_4, \\ c_E^1 &= [(1 - d_{14}) + (1 - d_{23})][(1 - d_{13}) + (1 - d_{24})]/P_4, \\ c_H^1 &= (1 - d_{14})(1 - d_{23})[(1 - d_{12}) + (1 - d_{34})]/P_4, \\ c_H^2 &= (1 - d_{13})(1 - d_{24})[(1 - d_{12}) + (1 - d_{34})]/P_4. \quad (3.36) \end{aligned}$$

This is again in complete agreement with refs. [4, 5].

3.5 Absence of Gram determinant ambiguities with 7 loops or less

The conjectured all-order symmetry (3.21) allows the R-charged correlators to be directly uplifted from the better-known integrands \mathcal{H}_{2222} , modulo the Gram ambiguities in eq. (3.23).

These ambiguities are restricted by the full permutation and conformal symmetries, and the condition that they originate from planar diagrams. We find that it is very difficult to write *planar* ambiguities.

An ambiguity in uplifting \mathcal{H}_{2222} can be characterized as a sum of planar conformal diagrams which vanishes when restricted to $d = 4$:

$$(\text{Gram ambiguity}) \equiv \sum c_i \mathcal{I}_i(X_1, \dots, X_{4+\ell}) \text{ which vanishes when } X_i \in \mathbb{R}^4 \quad (3.37)$$

where the c_i are pure numerical factors, and the \mathcal{I}_i are permutation-invariant conformal integrands in $\ell + 4$ arguments. Such functions were enumerated in ref. [2]. By evaluating the integrands numerically at several random points in $(\mathbb{R}^4)^{\ell+4}$ and computing the rank of the resulting matrix, we can then easily determine if a nontrivial combination c_i exists. In this way we proved that planar Gram determinants do not exist at least up to seven loops! That is, the conjecture (3.21) implies that:

$$\mathcal{H}^{(\ell)}(X_{ij}^2) = \mathcal{H}_{2222}^{(\ell)}(x_{ij}^2) \Big|_{x_{ij}^2 \rightarrow X_{ij}^2} \quad \text{for } \ell \leq 7. \quad (3.38)$$

The integrand \mathcal{H}_{2222} was given up to 10-loops in [3]. Up to 5-loops, we have verified that the prediction in eq. (3.38) is in perfect agreement with the results of [4, 5]. At 6 and 7 loops, the formula makes new predictions. At 8 loops, we do not know if a non-trivial Gram ambiguity actually exists, or not.

4 Octagons as scattering amplitudes on the Coulomb branch

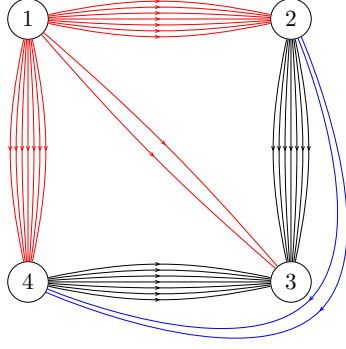
Correlators with large R -charge have been widely studied. They are a kind of “simplest four-point functions” which can be computed at finite-coupling using integrability. Using properties of the generating functional \mathcal{H} , in this section we show that they are closely related to scattering amplitudes on the Coulomb branch. This will be understood as a generalization of the correlator/amplitude duality.

We first discuss these relations at the integrand level. We will then observe that at generic location on the Coulomb branch, all integrals converge so the duality extends to integrated expression.

Octagons are defined in the literature by considering correlators with large R -charge so as to create four fat edges. This can be achieved using the polarizations shown in fig. 6. These polarized correlators can be extracted from the unpolarized ones by identifying the R -charge structure:

$$\begin{aligned} \lim_{K \rightarrow \infty} \langle \mathcal{O}_{2K+a}(x_1) \mathcal{O}_{2K+b}(x_2) \mathcal{O}_{2K+a}(x_3) \mathcal{O}_{2K+b}(x_4) \rangle \\ = (d_{12}d_{23}d_{34}d_{41})^K (d_{13})^a (d_{24})^b S_{a,b} + \dots \end{aligned} \quad (4.1)$$

where the dots stand for other R -charge structures which are projected out by our choice of polarizations.



$$O_1 = \text{Tr}(\bar{X}^{2K+a})$$

$$O_2 = \text{Tr}(X^K \bar{Z}^K \bar{Y}^b) + \text{cyclic permutations}$$

$$O_3 = \text{Tr}(Z^{2K} X^a) + \text{cyclic permutations}$$

$$O_4 = \text{Tr}(Z^K \bar{X}^K Y^b) + \text{cyclic permutations}$$

Figure 6: A family of simple four-point functions. The polarization choices ensure that a single Wick contraction exists in the field theory. K is assumed to be larger than loop order so as to make the four exterior bundles effectively uncrossable.

The “simplest correlator” $S_{a,b}$ is defined more precisely by taking the limit $K \rightarrow \infty$, which implies a factorization into two squares, referred to as octagons. In perturbation theory, this factorization is a consequence of the suppression of all planar Feynman diagrams that cross the square perimeter formed by the bridges of length K . Such a planar Feynman graph would contribute at the order $\sim (g^2)^K$ and hence can be neglected in the large charge limit.

Because S factorizes, it is natural to take its square root. This defines the *octagon*:

$$\mathbb{O} \times \mathbb{O} := \sum_{a,b \geq 0} d_{13}^a d_{24}^b S_{a,b}. \quad (4.2)$$

Let us express the integrand for $S_{a,b}$ in terms of the correlators $\mathcal{F}_{a,b}$ which we discussed above. Defining integrands similarly to eq. (2.4),

$$S_{a,b} = \sum_{\ell} \frac{(-g^2)^\ell}{\ell!} \int \frac{d^4 x_5}{\pi^2} \dots \frac{d^4 x_{4+\ell}}{\pi^2} \mathcal{S}_{a,b}^{(\ell)} \quad (4.3)$$

and comparing with eqs. (2.6) and (2.8), we get:

$$\mathcal{S}_{a,b}^{(\ell)} = 2x_{13}^2 x_{24}^2 \left(F_{a,b}^{(\ell)} - 2F_{a-1,b-1}^{(\ell)} + F_{a-2,b-2}^{(\ell)} \right) \quad \text{with } F_{a,b}^{(\ell)} \equiv \mathcal{F}_{\{\infty,a,\infty,\infty,b,\infty\}}^{(\ell)} \prod_{1 \leq i < j \leq 4} x_{ij}^2. \quad (4.4)$$

First we notice that all these R-charge structures contributing to the simplest correlators have ∞ exponents for the fat bridges $d_{12}, d_{23}, d_{34}, d_{41}$. Furthermore, by analyzing the generating function, we notice that these structures only received contributions from the terms in \mathbb{G} which contain all the four poles $(1 - d_{i,i+1})$, since only the geometric series of $\frac{1}{1-d_{i,i+1}}$ can give arbitrarily high exponents. We conclude that the octagon (squared) can be extracted at once by applying the null limit:

$$10\text{D null-square limit: } d_{i,i+1} \rightarrow 1 \equiv X_{i,i+1}^2 \rightarrow 0 \equiv y_{ij}^2 \rightarrow -x_{ij}^2 \quad (4.5)$$

$$\lim_{X_{i,i+1}^2 \rightarrow 0} G = \sum_{a,b,\ell} \left[\text{Diagram 1} \right] = \left[\text{Diagram 2} \right]^2$$

Figure 7: Extended correlator-amplitude duality: The generating function of all simplest correlators, obtained as the 10D null limit of G , is equal to the square of a four-point amplitude of massive particles in the Coulomb branch of $\mathcal{N} = 4$ SYM. On the left we sum over all diagonal bridges a and b and Lagrangian insertions; their coordinates x become region momenta on the right. The thick lines in the square perimeter represent the infinite R -charge. On the right the thick lines at the corners represent the four massive external particles and the thin lines are massless internal propagators.

to the generating function of all correlators G :

$$\mathbb{O} \times \mathbb{O} \Big|_{\text{integrand}} = 2 x_{13}^4 x_{24}^4 (1 - d_{13} d_{24})^2 \text{Res}_{X_{i,i+1}^2=0} \mathcal{H} \quad (4.6)$$

$$= \text{Res}_{d_{i,i+1}=1} G \Big|_{\text{integrand}} \quad (4.7)$$

where a residue is taken for each of the four propagators defining the 10D null square. The prefactor on the first line accounts for the three terms in eq. (4.4) and can be understood from $R_{1234} \rightarrow x_{13}^2 x_{24}^2 (1 - d_{13} d_{24})^2$ in eq. (2.7), which also explains why it cancels when we go back to the (unreduced) correlator. In the free theory, we find from eq. (3.14):

$$\mathbb{O}^{\text{free}} = \frac{1 - d_{13} d_{24}}{(1 - d_{23})(1 - d_{14})}. \quad (4.8)$$

Let us interpret this formula. When the y 's vanish, the residue in eq. (4.6) is similar to that entering the familiar (OPE-type) relation between the null limit of a correlation function and a Wilson loop (here, integrand) [19], which is itself dual to a gluon scattering amplitude [20–27]. While it is presently not obvious how to attach the y variables onto a Wilson loop, the amplitude side of that duality suggests a clear way forward. Namely, the y_i coordinates admit a natural physical interpretation as vacuum expectation values for the scalar fields of the $\mathcal{N} = 4$ theory [28]. Some of the gluons become massive through the Higgs mechanism, and the amplitude (integrands) for these massive W bosons are already known to enjoy a ten-dimensional dual conformal symmetry [29]. This suggests viewing the 10D null limit in

eq. (4.6) as a scattering amplitude of W bosons on the Coulomb branch:

$$\boxed{\frac{\mathbb{O}(x, y)}{\mathbb{O}^{\text{free}}(x, y)} = M(x, y)} \quad (4.9)$$

where now M is a massive four-particle amplitude in the Coulomb branch (normalized so that $M^{\text{free}} = 1$), with external momenta and masses satisfying:

$$p_i^\mu \equiv x_{i,i+1}^\mu \quad \text{and} \quad m_i^2 \equiv y_{i,i+1}^2. \quad (4.10)$$

The 10D null-limit $X_{ij}^2 \rightarrow 0$ is then simply the on-shell condition on the Coulomb branch: $p_i^2 + m_i^2 = 0$. The duality is depicted in fig. 7.

In other words, we propose that the octagon is precisely a scattering amplitude on the Coulomb branch.

The octagons defined in this paper span only a restricted subset of the Coulomb branch, where each Higgs vev satisfies $y_i^2 = 0$. (Nonzero external masses $y_{i,i+1}^2 \neq 0$ can still be realized by allowing the y_i to be complex 6-vectors.) This suggests the existence of a more general, truly ten-dimensional object which relaxes the constraint $y_i^2 = 0$, but this seems difficult to capture using local operators in the field theory and is beyond the scope of this paper.

4.1 Example amplitudes on the restricted Coulomb branch

Let us first exemplify these relations at the integrand level by present them up to three loops. We start with the integrand for stress tensors in eqs. (2.11) to (2.13), then uplift to the generating function G using (3.23), (3.31) and take the 10D null-limit to get \mathbb{O} or equivalently the amplitude (4.6):

$$\begin{aligned} M = & 1 - g^2 X_{13}^2 X_{24}^2 g_{1234} \\ & + g^4 \left[\frac{X_{13}^2 (X_{24}^2)^2}{x_{24}^2} h_{13;24} + \frac{(X_{13}^2)^2 X_{24}^2}{x_{13}^2} h_{24;13} \right] \\ & - g^6 \left[\frac{X_{13}^2 (X_{24}^2)^3}{(x_{24}^2)^2} L_{13;24} + \frac{(X_{13}^2)^3 X_{24}^2}{(x_{13}^2)^2} L_{24;13} + \frac{X_{13}^2 (X_{24}^2)^2}{x_{24}^2} (T_{13;24} + T_{13;42}) \right. \\ & \left. + \frac{(X_{13}^2)^2 X_{24}^2}{x_{13}^2} (T_{24;13} + T_{24;31}) \right] + \mathcal{O}(g^8). \end{aligned} \quad (4.11)$$

The square root of $\mathbb{O} \times \mathbb{O}$ was computed directly at integrand level by dropping graphs with vertices on the ‘‘reverse side’’ of the square. The dual graphs corresponding to the integrand in eq. (4.11) are shown in fig. 8. The extra factors x_{ij}^2 in the denominators are there for consistency with the normalization of the ladders (g and h) in (2.16) and the 3-loop ladder (L) and tennis-court (T) in (A.1).

The above integrand agrees precisely with that entering the gluon scattering amplitude, with precisely the same coefficients [30]. The fact that the correct Coulomb branch integrand is obtained from the massless case by simply making all distances ten-dimensional (ie. $x_{13}^2 \mapsto$

Figure 8: Conformal integrals in the four-particle amplitude integrand up to 3 loops. The first line shows one-loop, two-loop and three-loop ladder integrals in momentum space representations. The last line illustrates, for the three-loop tennis-court integral, the planar graph duality which relates the momentum and position space representations.

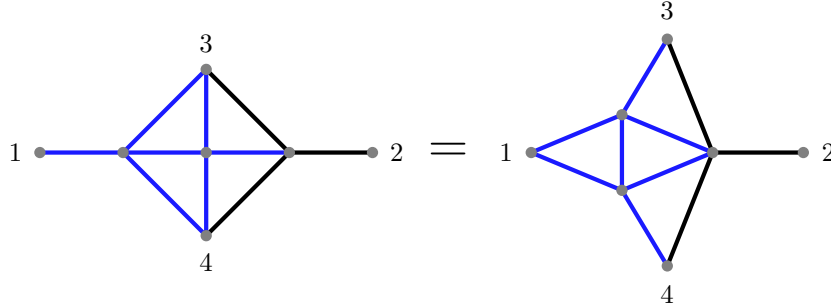


Figure 9: Conformal magic identity: the three-loop ladder (left panel) and the tennis court (right panel) can be shown to be identical off-shell by using the conformal invariance of the highlighted two-loop ladder sub-integral.

$X_{13}^2 \equiv x_{13}^2 + y_{13}^2$, $x_{24}^2 \mapsto X_{24}^2$ in the numerator) is also in agreement with existing results in the scattering amplitudes context [28]. Within the restricted Coulomb branch on which the octagon is defined, only those two invariants have a nontrivial 10D component.

On the restricted Coulomb branch, the *external* masses $-x_{i,i+1}^2 = y_{i,i+1}^2$ are still generically nonvanishing, which makes the amplitude effectively off-shell from the four-dimensional perspective. This has an important implication: there are no divergences and conformal symmetry of integrated octagons is unbroken (from the amplitude perspective, this is called dual conformal symmetry). In particular, the conformal “magic” identities of ref. [31] hold exactly

	Correlator		Amplitude
$10D :$	$G(X)$	$\xrightarrow{X_{i,i+1}^2 \rightarrow 0}$	$[M(x, y)]^2$
	$\downarrow y_{ij}^2 \rightarrow 0$		$\downarrow y_{ij}^2 \rightarrow 0$
$4D :$	$G_{2222}(x)$	$\xrightarrow{x_{i,i+1}^2 \rightarrow 0}$	$[M(x, 0)]^2$

Figure 10: Relationship between the massive (top) and massless (bottom) correlator-amplitude duality. All arrows commute at integrand level. The different massless limits are however not equivalent at the integrated level.

on our setup! For example (see fig. 9):

$$T_{13;24} = L_{13;24} = L_{24;13}. \quad (4.12)$$

The integrated form of the three-loop gluon scattering amplitude on the restricted Coulomb branch amplitude can thus be written very simply:

$$\begin{aligned}
M = & 1 - g^2 (1 - d_{13})(1 - d_{24}) x_{13}^2 x_{24}^2 g_{1234} \\
& + g^4 (1 - d_{13})(1 - d_{24}) (2 - d_{13} - d_{24}) x_{13}^2 x_{24}^2 h_{13;24} \\
& - g^6 (1 - d_{13})(1 - d_{24}) [(1 - d_{13})^2 + (1 - d_{24})^2 + 2(2 - d_{13} - d_{24})] x_{13}^2 x_{24}^2 L_{13;24} \\
& + \mathcal{O}(g^8). \quad (4.13)
\end{aligned}$$

These functions are given in eqs. (2.16) and (A.1). The integrated 10D null octagon is identical up to the factor $\mathbb{O}^{\text{free}} = \frac{1-d_{13}d_{24}}{(1-d_{13})(1-d_{24})}$ (see eq. (4.9)).

At higher loops, new, harder integrals appear. On the other hand, the octagon was calculated exactly using integrability. In the next section we leverage these results to predict new scattering amplitudes and Feynman integrals.

4.2 Comments on the four-dimensional massless limit

In fig. 10 we contrast and relate our new duality between the generating function G and the coulomb branch amplitude, eqs. (4.6) and (4.9), with the well-known duality between the correlator of stress tensors and the four-gluon amplitude. At the integrand level, that duality takes formally the same form [32]

$$\lim_{x_{i,i+1}^2 \rightarrow 0} \frac{\mathcal{G}_{2222}(x_i)}{\mathcal{G}_{2222}^{\text{free}}} = M(x_i)^2 \quad (y = 0). \quad (4.14)$$

In the massless case, however, the loop integrals diverge and as a result the relation at integrated level takes on a more complicated form:

$$\lim_{x_{i,i+1}^2 \rightarrow 0} \frac{G_{2222}(x_i)}{G_{2222}^{\text{free}}} = \lim_{\varepsilon \rightarrow 0} f(\{\mu_{\text{IR}}^2 x_{i,i+1}^2\}, x_{13}^2, x_{24}^2, \varepsilon) [M(p_i)]^2 \quad (y=0) \quad (4.15)$$

where f is a universal function which converts the different regularizations. For example, if dimensional regularization is used on the scattering amplitude side, the relation to the $x_{i,i+1}^2 \rightarrow 0$ limit of the correlator was worked out in refs. [19, 27].

An interesting feature of our novel correlator/amplitude duality (4.6) is that, since the integrals are finite (as long as all $y_{i,i+1}^2 \neq 0$), it translates directly to the integrated level! This is what we have used in eq. (4.13) above.

As an alternative to dimensional regularization, regularization of scattering amplitudes using the Coulomb branch has been studied starting from [28]. In the simplest setup, one turns on a vev to only one of the six scalars, in such a way as to give masses to the outermost internal propagators of the amplitude as represented in the top of fig. 11. In this limit, one finds a mass-regularized version of the BDS Ansatz [28, 33]:

$$\begin{aligned} \log M(x, 0) = & -\frac{\Gamma_{\text{cusp}}(g)}{4} \left[2 \log \left(\frac{m^2}{x_{13}^2} \right) \log \left(\frac{m^2}{x_{24}^2} \right) - \pi^2 \right] \\ & + \tilde{\mathcal{G}}(g) \left[\log \left(\frac{m^2}{x_{13}^2} \right) + \log \left(\frac{m^2}{x_{24}^2} \right) \right] + \tilde{c}(g) + \mathcal{O}(m^2), \end{aligned} \quad (4.16)$$

where

$$\Gamma_{\text{cusp}}(g) = 4g^2 - 8\zeta_2 g^4 + 88\zeta_4 g^6 - (876\zeta_6 + 32\zeta_3^2) g^8 + \mathcal{O}(g^{10}). \quad (4.17)$$

These kinematics however do not overlap with the restricted Coulomb graph, on which $y_i^2 = 0$. The result is thus to be contrasted with the massless limit of the octagon, in which the *internal* masses are set to zero first and in which one finds a different kind of exponentiation [7, 34]²:

$$\begin{aligned} \lim_{x_{i,i+1}^2, d_{13}, d_{24} \rightarrow 0} \log M &= \lim_{x_{i,i+1}^2, d_{13}, d_{24} \rightarrow 0} \log \mathbb{O} \\ &= -\frac{\Gamma_{\text{oct}}(g)}{16} \log^2 \left(\frac{x_{12}^2 x_{23}^2 x_{34}^2 x_{41}^2}{(x_{13}^2 x_{24}^2)^2} \right) - \frac{g^2}{4} \log^2 \left(\frac{x_{12}^2 x_{34}^2}{x_{23}^2 x_{41}^2} \right) - \frac{1}{2} D_0(g), \end{aligned} \quad (4.18)$$

where

$$\Gamma_{\text{oct}}(g) = \frac{2}{\pi^2} \log \cosh(2\pi g) \stackrel{g \rightarrow 0}{=} 4g^2 - 16\zeta_2 g^4 + 256\zeta_4 g^6 - 3264\zeta_6 g^8 + \mathcal{O}(g^{10}). \quad (4.19)$$

We see that not all massless limits of scattering amplitudes are controlled by Γ_{cusp} ! It would be interesting to understand how to interpolate between these approaches to the massless limit.

²The one-loop exact term is only valid at weak coupling, while at strong coupling it gets modified to become linear in g .

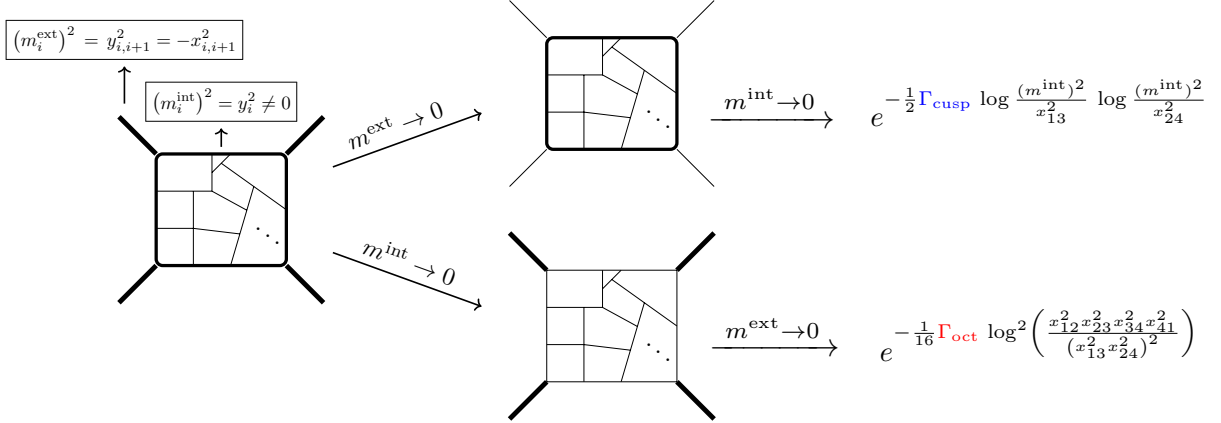


Figure 11: Different massless limits of Coulomb branch amplitudes lead to very different exponential behavior. Both objects in the middle column are infrared-safe.

5 A Coulomb branch amplitude from integrability

An alternative to the hard problem of evaluating high-loop order conformal integrals is to use the hexagonalization of [18] to find the four-point functions analytically. This is an integrability-based method which provides a finite-coupling prescription to compute correlation functions. In this section we use this method to provide a finite-coupling result for the generating function of simplest correlators which, through the duality (4.9), also gives the coulomb branch amplitude. Our result is given in terms of the octagon form factors \mathbb{O}_l , introduced in [6, 7] and vastly studied at weak, strong and finite coupling in [8, 9, 34–40]. Furthermore, we consider the weak coupling limit of the octagons and compare it with the integrand of the coulomb branch amplitude, which can be found up to ten loops thanks to the $10D$ uplift (3.23) of the four-gluon integrand given in [3]. This allows us to find a map between simple analytic functions and linear combinations of conformal integrals, most of them unknown at the function level.

5.1 Hexagonalization and octagons

Hexagonalization [18, 41] proposes an uplift from the free theory to the finite-coupling correlator by dressing the free theory graphs with hexagons [42] as shown in fig. 12. According to ref. [18]:

$$G = \sum_{\{l_{ij}\}} c_{\{l_{ij}\}} \underbrace{\prod_{(i,j)} (d_{ij})^{l_{ij}}}_{\text{free Wick contractions}} \left[\sum_{\{\psi_{ij}\}} \prod_{(i,j)} \mu_{\psi_{ij}} e^{-E_{\psi_{ij}} l_{ij}} \mathcal{W}_{\psi_{ij}} \prod_{(i,j,k)} \mathcal{H}_{\psi_{ij}, \psi_{jk}, \psi_{ki}} \right] \quad (5.1)$$

where we consider a sum over all positive bridges $l_{ij} > 0$ to account for all possible charges and obtain the generating function G of all four-point functions.

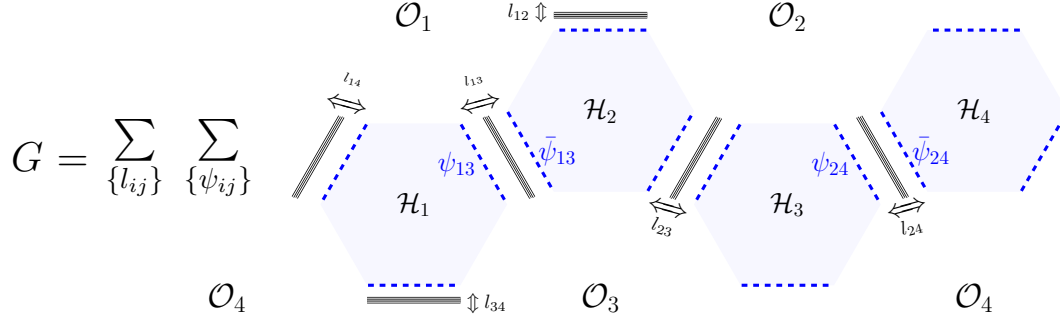


Figure 12: Hexagonalization: finite-coupling correlators are obtained from the sum over the free theory graphs (skeleton graphs) labeled by the six bridges $\{l_{ij}\}$, tessellated into four hexagons $\mathcal{H}_{\psi_{ij}, \psi_{jk}, \psi_{ki}}$ which are glued by sums over complete basis of mirror states $\{\psi_{ij}\}$ that propagate traversing the bridges. The unrestricted sum over all non-negative integers l_{ij} give the sum G of all four-point planar correlators.

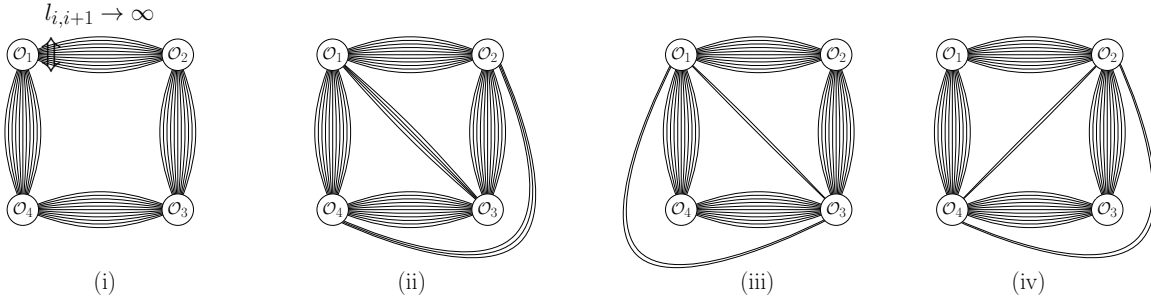


Figure 13: The four types of skeleton graphs contributing to the large R-charge correlators or 10D null limit. All graphs have a square perimeter with bridges of infinite length and they are distinguished by the position and length of their diagonal bridges.

In principle, all the ingredients in (5.1) are known at finite coupling, allowing to perform the infinite sum and obtain G . However, in practice this is a complicated task which first requires dealing with the involved matrix structure of the hexagon form factors $\mathcal{H}_{\psi_{ij}, \psi_{jk}, \psi_{ki}}$ for generic mirror states ψ_{ij} ³. Fortunately this procedure simplifies when taking the 10D null limit since this only receives contributions from skeleton graphs with large R-charges in their perimeter, see fig. 13. For these graphs the sum over states propagating on the bridges with infinite length $l_{12}, l_{23}, l_{34}, l_{41}$ projects to the vacuum state thanks to the exponentially suppressed factor in (5.1). This results on a factorization into two building blocks that we call octagons.

The octagon form factor is composed by a pair of hexagons separated by a diagonal bridge l and glued by a sum over a complete basis of mirror states propagating on this bridge.

³see for instance [43, 44] for resummations at strong coupling in the context of three-point functions and see [45–47] for examples on more generic hexagon form factors in the context of four- and five-point functions at weak coupling.

Schematically we represent it as:

$$\text{Octagon}_l(z, \bar{z}, \alpha, \bar{\alpha}) = \sum_{\psi} \text{Diagram} \quad (5.2)$$

Explicit finite-coupling expressions for this octagon form factor can be found in [6] in terms of the spacetime (z, \bar{z}) and R-charge $(\alpha, \bar{\alpha})$ cross-ratios defined as in (2.17). We review some of these representations in section 5.2.1. We are interested in the 10D null limit obtained by simply setting $y_{i,i+1}^2 = -x_{i,i+1}^2$:

$$\begin{aligned} \mathbb{O}_l &= \lim_{d_{i,i+1} \rightarrow 1} \text{Octagon}_l(z, \bar{z}, \alpha, \bar{\alpha}) \\ &= \text{Octagon}_l(z, \bar{z}, \alpha_*, \bar{\alpha}_*), \end{aligned} \quad (5.3)$$

where the R-charge cross-ratios solve the equations: $\frac{\alpha_* \bar{\alpha}_*}{z \bar{z}} = \frac{(1-\alpha_*)(1-\bar{\alpha}_*)}{(1-z)(1-\bar{z})} = \frac{1}{d_{13} d_{24}}$. The object \mathbb{O}_l serves as a building block to compute our 10D null octagon as the sum:

$$\mathbb{O} = \mathbb{O}_0 + \sum_{l=1}^{\infty} (d_{13})^l \mathbb{O}_l + (d_{24})^l \mathbb{O}_l. \quad (5.4)$$

This result has the structure dictated by hexagonalization: each tree level graph, represented by the diagonal propagators, gets dressed by the building block \mathbb{O}_l .

It is instructive to verify that squaring this expression reproduces the generating function of all simplest correlators, which can be organized following the rules of hexagonalization as:

$$\begin{aligned} \mathbb{O} \times \mathbb{O} &= \sum_{l_{13}, l_{24}=0}^{\infty} (d_{13})^{l_{13}} (d_{24})^{l_{24}} \left(\delta_{l_{13},0} \delta_{l_{24},0} \mathbb{O}_0 \mathbb{O}_0 + 2(1 - \delta_{l_{13},0})(1 - \delta_{l_{24},0}) \mathbb{O}_{l_{13}} \mathbb{O}_{l_{24}} \right. \\ &\quad \left. + (1 - \delta_{l_{13},0}) \delta_{l_{24},0} \sum_{m=0}^{l_{13}} \mathbb{O}_m \mathbb{O}_{l_{13}-m} + \delta_{l_{13},0} (1 - \delta_{l_{24},0}) \sum_{m=0}^{l_{24}} \mathbb{O}_m \mathbb{O}_{l_{24}-m} \right). \end{aligned} \quad (5.5)$$

This is an example of ‘‘octogonalization’’: the four terms in the sum (5.5) are associated to the four types of skeleton graphs, listed in fig. 13, dressed by a pair of octagons \mathbb{O}_l . The first term corresponds to the case without diagonal bridges $l_{13} = l_{24} = 0$ in fig. 13 (i). The second term has both non-zero diagonals $l_{13}, l_{24} \neq 0$, hence the accompanying factor of 2 corresponding to the swapping of the bridges positions between the inside and the outside of the square frame in the graph (ii). Finally, the third and fourth terms correspond to the graphs (iii) and (iv) which have a single non-zero diagonal bridge, $l_{13} \neq 0, l_{24} = 0$ and $l_{13} = 0, l_{24} \neq 0$ respectively. This condition allows the single diagonal bundle to split between the inside and outside of the square frame while still respecting planarity and explains the sums in the bottom line of (5.5).

Thanks to the duality (4.9), our integrability-based result for the 10D null octagon (5.4) provides a finite coupling representation of a finite Coulomb branch amplitude in terms of \mathbb{O}_l . This allows for a thorough study of the amplitude in various regimes of the coupling and kinematics using the results in [6–9, 34–40]. In this paper we follow a different route and take advantage of the knowledge of the amplitude integrand M up to 10 loops and compare it with the results from integrability in the weak coupling limit. For this purpose, in what follows we review the representations of the octagon form factor and its weak coupling limit.

5.2 The octagon from integrability: 10D null limit and weak coupling expansion

In [6], using integrability, the octagon form factor with bridge l was found as a sum over mirror states:

$$\text{Octagon}_l(z, \bar{z}, \alpha, \bar{\alpha}) = 1 + \sum_{n=1}^{\infty} \chi_n(z, \bar{z}, \alpha, \bar{\alpha}) I_{n,l}(z, \bar{z}) \quad (5.6)$$

where n stands for the number of mirror particles. This n -particle contributions can be decomposed into a rational factor χ_n carrying all the R -charge dependence and the n -particle integrals $I_{n,l}$ depending only on the spacetime cross ratios. Explicit representations for these components, at finite coupling, can be found in [6]. Here it only suffices to know the 10D null limit:

$$\lim_{d_{i,i+1} \rightarrow 1} \chi_n = (1 - d_{13}d_{24})^n \quad (5.7)$$

to obtain:

$$\mathbb{O}_l(z, \bar{z}, d_{13}, d_{24}) = 1 + \sum_{n=1}^{\infty} (1 - d_{13}d_{24})^n I_{n,l}(z, \bar{z}). \quad (5.8)$$

An alternative and more efficient way to calculate the octagon is through the determinant of an infinite matrix [8, 9, 34, 37–40]:

$$\mathbb{O}_l = \det(1 - \mathbb{K}_l) \quad (5.9)$$

whose elements are given by integrals of Bessel functions of the first kind:

$$(\mathbb{K}_l)_{ij} = 2(-1)^{i-j}(2j + l - 1) \int_0^{\infty} d\tau \chi(\tau) \frac{J_{2i+l-1}(2g\tau) J_{2j+l-1}(2g\tau)}{\tau} \quad (5.10)$$

where $i, j \geq 1$ and only the weight factor $\chi(\tau)$ depends on the spacetime and R -charge cross ratios. In our 10D null limit this weight factor becomes effectively:

$$\chi(\tau) = \frac{(1 - d_{13}d_{24})}{\sqrt{z\bar{z}(1-z)(1-\bar{z})}} \frac{1}{\cosh(\sqrt{\zeta^2 + \tau^2}) - \cos \phi}, \quad \text{with } e^{-2\zeta} = \frac{z\bar{z}}{(1-z)(1-\bar{z})}, \quad e^{2i\phi} = \frac{z(1-\bar{z})}{\bar{z}(1-z)}. \quad (5.11)$$

The integrals in (5.10) can be easily evaluated at weak coupling as we now review.

5.2.1 Octagon at weak coupling

In this regime, the infinite matrix \mathbb{K}_l can be truncated to a matrix of dimension $\frac{\ell-l}{2}$ when interested in the ℓ -loop order. This is because the Bessel functions scale as $J_n(g\tau) \propto (g\tau)^n$. Furthermore, the integral over τ can be easily performed order by order in the coupling: the integration of $\chi(\tau)\tau^{2n-1}$ is proportional to the well-known ladder integral F_n . These functions were introduced in [48] as:

$$F_p(z, \bar{z}) = (-1) \sum_{j=p}^{2p} \frac{j! \left[-\log\left(\frac{z}{z-1} \frac{\bar{z}}{\bar{z}-1}\right) \right]^{2p-j}}{p!(j-p)!(2p-j)!} \left[\frac{\text{Li}_j\left(\frac{z}{z-1}\right) - \text{Li}_j\left(\frac{\bar{z}}{\bar{z}-1}\right)}{z - \bar{z}} \right]. \quad (5.12)$$

In this basis, the expansion of the matrix elements goes as:

$$(\mathbb{K}_l)_{ij} = \sum_{\ell=i+j+l-1}^{\infty} C_{l;i,j}^{(\ell)} (-g^2)^\ell (1 - d_{13}d_{24}) F_\ell \quad (5.13)$$

with coefficients:

$$C_{l;i,j}^{(\ell)} = \frac{(-1)^{l+1} (2j+l-1)(2\ell)! \ell! (\ell-1)!}{(\ell - (i+j+l-1))! (\ell + (i+j+l-1))! (\ell - |i-j|)! (\ell + |i-j|)!}. \quad (5.14)$$

The coefficient of $(1 - d_{13}d_{24})^n$ can thus be loop-expanded as:

$$I_{n,l} = \sum_{\ell=n(n+l)}^{\infty} (-g^2)^\ell I_{n,l}^{(\ell)} \quad (5.15)$$

where each loop correction is a sum of products of n ladder integrals. The basis of such products can be further refined: they only appear in combinations such that the double discontinuity around $z \rightarrow \infty$ vanishes.⁴ This forces the ladders to appear in determinants which generalize those in the so-called fishnet diagrams [49]. A basis of such determinants was introduced in [7] as:

$$F_{i_1, i_2, \dots, i_n} = \prod_{m=1}^n \frac{1}{i_m!(i_m-1)!} \begin{vmatrix} f_{i_1} & f_{i_2-1} & \cdots & f_{i_n-n+1} \\ f_{i_1+1} & f_{i_2} & \cdots & f_{i_n-n+2} \\ \vdots & \vdots & \ddots & \vdots \\ f_{i_1+n-1} & f_{i_2+n-2} & \cdots & f_{i_n} \end{vmatrix} \quad \text{with } f_p = p!(p-1)! F_p \quad (5.16)$$

and the diagonal elements are dictated by the subscripts in F_{i_1, i_2, \dots, i_n} . Under this definition, the elements of our basis with a single index coincide with the standard ladder integral (5.12).

Using this basis, the ℓ -loop contribution can be written as a sum of determinants with ℓ indices and strong restrictions:

$$I_{n,l}^{(\ell)} = (-1)^{nl} \times \sum_{\substack{i_1 + \dots + i_n = \ell \\ \text{with } (i_{p+1} - i_p) \geq 2 \text{ and } i_1 > l}} c_{l; \{i\}_n} F_{i_1, i_2, \dots, i_n}. \quad (5.17)$$

⁴This property can be seen directly from eq. (5.10) because monodromy around $z \rightarrow \infty$ shifts \mathbb{K}_{ij} by the residue of a pole at the value t_* where the denominator of $\chi(t)$ vanishes. This residue is a matrix of rank one.

$\ell \backslash l$	\mathbb{O}_0	\mathbb{O}_1	\mathbb{O}_2
1	F_1	0	0
2	$2F_2$	$-F_2$	0
3	$6F_3$	$-4F_3$	F_3
4	$20F_4 + F_{1,3}$	$-15F_4$	$6F_4$
5	$70F_5 + 6F_{1,4}$	$-56F_5$	$28F_5$
6	$252F_6 + 28F_{1,5} + \frac{18}{5}F_{2,4}$	$-210F_6 + F_{2,4}$	$120F_6$
7	$924F_7 + 120F_{1,6} + 24F_{2,5}$	$-792F_7 + 8F_{2,5}$	$495F_7$
8	$3432F_8 + 495F_{1,7} + \frac{855}{7}F_{2,6} + \frac{162}{7}F_{3,5}$	$-3003F_8 + 45F_{2,6} + 11F_{3,5}$	$2002F_8 + F_{3,5}$
9	$12870F_9 + 2002F_{1,8} + 561F_{2,7} + \frac{2325}{14}F_{3,6} + F_{1,3,5}$	$-11440F_9 + 220F_{2,7} + \frac{600}{7}F_{3,6}$	$8008F_9 + 10F_{3,6}$

Table 1: Octagons up to nine loops for bridges $l = 0, 1, 2$. In order to restore the coupling and 10D character we make the rescaling $F_{i_1, \dots, i_n} \rightarrow (-g^2)^{i_1 + \dots + i_n} (1 - d_{13}d_{24})^n F_{i_1, \dots, i_n}$. We highlight the single-determinant cases given by the close formulas (5.19)-(5.20).

The coefficients $c_{l; \{i\}_n}$ are positive rational numbers for which we have not found a closed form expression, except for the one-particle case:

$$I_{n=1,l}^{(\ell)} = (-1)^l \binom{2\ell - 2}{\ell - l - 1} F_\ell. \quad (5.18)$$

In [7] it was shown how to fix all coefficients $c_{l; \{i\}_n}$ for arbitrary n and bridge $l = 0$ following a bootstrap approach that uses special kinematic limits of \mathbb{O}_0 . Unfortunately, we lack a bootstrap method to fix the coefficients with $l > 0$. For these we resort to a direct loop expansion of the integrability results.

In table 1 we show all non-vanishing loop corrections below 9 loops. Furthermore, by performing expansions up to 25 loops ($n(n+l) \leq 25$), we have identified that the leading and sub-leading loop contributions for arbitrary n and l are each given by a single determinant. The leading term is:

$$I_{n,l}^{[n(n+l)]} = (-1)^{n l} F_{1+l, 3+l, \dots, 2n-1+l} \quad (5.19)$$

and the subleading term carries the same indexes except for the last one which is shifted by one unit:

$$I_{n,l}^{[n(n+l)+1]} = (-1)^{n l} 2(2n - 1 + l) F_{1+l, 3+l, \dots, 2n-1+l+1}. \quad (5.20)$$

These leading and subleading corrections will be mapped to scattering amplitude integrals shortly.

5.3 Integrals from octagons

In this section we compare the representation of the coulomb branch amplitude given by conformal integrals against the integrability representation of the octagon. The integrand can be obtained in either of two ways: by taking the 10D null limit of the correlation function integrand from eq. (3.38), or alternatively, by uplifting to 10-dimensions directly the known integrand for massless gluon amplitudes using the same procedure:

$$M(x, y) \Big|_{\text{integrand}} = M(x, 0) \Big|_{x_{13}^2 \mapsto X_{13}^2, x_{24}^2 \mapsto X_{24}^2}. \quad (5.21)$$

As noted, this uplift is unambiguous up to and including at least seven loops, where Gram determinants ambiguities were shown above to be absent.

Integrated expressions for M on the other hand follow directly from our new conjectured amplitude/correlator duality (4.9) and the computation of the octagon \mathbb{O} using integrability:

$$M = \frac{\mathbb{O}}{\mathbb{O}^{\text{free}}} = 1 + (1 - d_{13})(1 - d_{24}) \sum_{l=0}^{\infty} \frac{(d_{13})^l + (d_{24})^l}{1 + \delta_{l,0}} \sum_{n=1}^{\infty} (1 - d_{13}d_{24})^{n-1} I_{n,l} \quad (5.22)$$

where we made use of (5.8) and the free limit: $\mathbb{O}^{\text{free}} = 1 + \sum_{l=1}^{\infty} (d_{13})^l + (d_{24})^l = \frac{1-d_{13}d_{24}}{(1-d_{13})(1-d_{24})}$.

To compare these two formulas, it is helpful to group terms with different dependence on d_{13} and d_{24} :

$$M = 1 + \sum_{a,b \geq 1} (1 - d_{13})^a (1 - d_{24})^b M_{a,b}. \quad (5.23)$$

Using the formulas recorded in (4.11), we can readily check the agreement up to three loops:

$$\begin{aligned} M_{1,1} &= -g^2 x_{13}^2 x_{24}^2 g_{1234} &&= -g^2 F_1, && (5.24) \\ M_{1,2} &= g^4 x_{13}^2 x_{24}^2 h_{13;24} - g^6 x_{13}^2 x_{24}^2 (T_{13;24} + T_{13;42}) + \mathcal{O}(g^8) &&= g^4 F_2 - 2g^6 F_3 + \mathcal{O}(g^8), \\ M_{2,1} &= g^4 x_{13}^2 x_{24}^2 h_{24;13} - g^6 x_{13}^2 x_{24}^2 (T_{24;13} + T_{24;31}) + \mathcal{O}(g^8) &&= g^4 F_2 - 2g^6 F_3 + \mathcal{O}(g^8), \\ M_{1,3} &= -g^6 x_{13}^2 x_{24}^2 L_{13;24} + \mathcal{O}(g^8) &&= -g^6 F_3 + \mathcal{O}(g^8), \\ M_{3,1} &= -g^6 x_{13}^2 x_{24}^2 L_{24;13} + \mathcal{O}(g^8) &&= -g^6 F_3 + \mathcal{O}(g^8). \end{aligned} \quad (5.25)$$

All integrated expressions satisfy the symmetry $M_{a,b} = M_{b,a}$, which is a simple consequence of conformal invariance since all cross-ratios are invariant [31]. Note that $M_{1,1}$ is one-loop exact: this is easy to understand from the scattering amplitude picture (all conformal integrals with $\ell \geq 2$ loops require more powers of x_{13}^2 or x_{24}^2 in the numerators).

In general, by equating (5.22) with (5.23) we find the following expression for the partial amplitudes $M_{a,b}$ in terms of the n -particle integrability contributions $I_{n,l}$:

$$M_{a,b} = \sum_{n=\min(a,b)}^{a+b-1} \sum_{\substack{l \geq 0 \\ l+n \geq a,b}}^{\infty} C_{a,b}^{n,l} I_{n,l} \quad (5.26)$$

with

$$C_{a,b}^{n,l} = \frac{(-1)^{a+b-n-1}}{1 + \delta_{l,0}} \left[\binom{n-1}{a-1} \binom{a+l-1}{a+b-n-1} + (a \leftrightarrow b) \right]. \quad (5.27)$$

While eq. (5.26) is valid at finite coupling, here we will only study it order by order in the coupling g^2 . We have seen in eq. (5.17) that the right-hand-side, to all orders in the coupling, is a sum of determinants of ladder integrals. This is far from obvious from the integrals on the left-hand-side and this predicts new integral relations.

The simplest case corresponds to $M_{1,1}$ where only $n = 1$ particles contribute in eq. (5.26):

$$M_{1,1} = I_{1,0} + 2 \sum_{l=1}^{\infty} I_{1,l}. \quad (5.28)$$

The infinite sum from integrability agrees nontrivially with the one-loop exact result $M_{1,1} = g^2 f_1$ quoted in eq. (5.24).

Groups $M_{a,b}$ with $b \geq 2$ receive contributions from two-particle integrals, starting from high-enough loop order. For instance for $a = 1$ we have:

$$M_{1,b} = (-1)^{b-1} \underbrace{\left[(-g^2)^b I_{1,b-1}^{(b)} + (-g^2)^{b+1} \left(I_{1,b-1}^{(b+1)} + b I_{1,b}^{(b+1)} \right) + \dots \right]}_{\text{single-particle}} + (-g^2)^{2b} I_{2,b-2}^{(2b)} + \mathcal{O}(g^{4b+2}) \quad (5.29)$$

where the upper parenthesis $I^{(\ell)}$ denote the coefficient of $(-g^2)^\ell$. From the viewpoint of the scattering amplitudes, the leading term is simply a single ladder integral:

$$M_{1,b}^{(b)} = x_{13}^2 (x_{24}^2)^b \quad \begin{array}{c} 1 \\ \boxed{ } \\ \leftarrow \rightarrow \\ b \end{array} \quad {}^2 = F_b. \quad (5.30)$$

The ladder integrals were famously computed long ago [48] and one might say that our duality provides one (more) re-derivation through integrability.

The single-particle contributions can be projected out by considering partial amplitudes with $a, b \geq 2$. The leading contribution sets in at order $M_{a,b} \sim g^{2ab}$ where the integrand is simply the fishnet integral of ref. [49, 50] which will be discussed below. Both the leading and subleading term are given by a single term with $n = a$ and $l = b - a$ in the integrability formula:

$$M_{a,b} = (-g^2)^{ab} I_{a,b-a}^{(ab)} + (-g^2)^{ab+1} I_{a,b-a}^{(ab+1)} + \mathcal{O}(g^{2(ab+2)}) \quad \text{with } b \geq a \geq 2. \quad (5.31)$$

Interestingly, each of these evaluates to a single determinant of ladder integrals, see eq. (5.20). The contributing amplitude integrals are nontrivial and will be discussed below.

5.3.1 Detailed comparison at four-loops

The comparison between Feynman integrals and integrability becomes particularly interesting starting from four-loops: non-ladder integrals appear at the same time as multi-particle contributions.

Evaluating the amplitude (5.26) using the integrability results quoted in eqs. (5.18) and (5.19) we find the following predictions:

$$\begin{aligned} M_{4,1}^{(4)} &= -I_{1,3}^{(4)} &= F_4, \\ M_{3,1}^{(4)} &= I_{1,2}^{(4)} + 3I_{1,3}^{(4)} &= 3F_4, \\ M_{2,1}^{(4)} &= -I_{1,1}^{(4)} - 2I_{1,2}^{(4)} - 3I_{1,3}^{(4)} + I_{2,0}^{(4)} &= 6F_4 + F_{1,3}, \\ M_{2,2}^{(4)} &= -I_{2,0}^{(4)} &= -F_{1,3}, \end{aligned} \quad (5.32)$$

where $F_{1,3} = \frac{1}{12} \begin{vmatrix} f_1 & f_2 \\ f_2 & f_3 \end{vmatrix}$ is the simplest determinant of ladders.

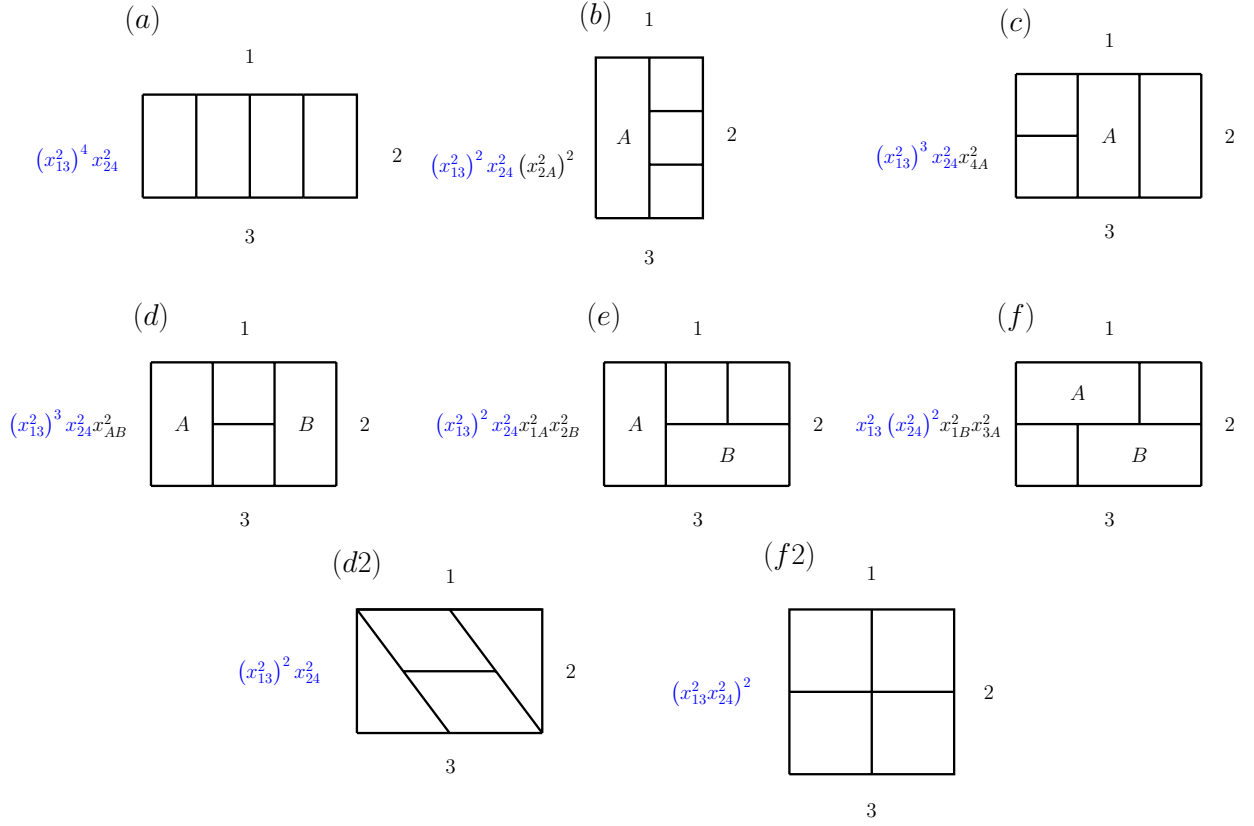


Figure 14: Four-loop integrals entering eq. (5.33) in scattering amplitude notation.

The same amplitudes are also expressed as the following Feynman integrals [51], shown in fig. 14:

$$\begin{aligned}
M_{4,1}^{(4)} &= \mathcal{I}_{1,2,3,4}^{(4)a}, \\
M_{3,1}^{(4)} &= \left(\mathcal{I}_{1,2,3,4}^{(4)c} + \mathcal{I}_{1,4,3,2}^{(4)c} \right) + \mathcal{I}_{1,2,3,4}^{(4)d}, \\
M_{2,1}^{(4)} &= \left(\mathcal{I}_{1,2,3,4}^{(4)b} + \mathcal{I}_{1,4,3,2}^{(4)b} \right) + \left(\mathcal{I}_{1,2,3,4}^{(4)e} + \mathcal{I}_{1,4,3,2}^{(4)e} + \mathcal{I}_{3,2,1,4}^{(4)e} + \mathcal{I}_{3,4,1,2}^{(4)e} \right) - \left(\mathcal{I}_{1,2,3,4}^{(4)d2} + \mathcal{I}_{1,4,3,2}^{(4)d2} \right), \\
&\quad + \left(\mathcal{I}_{2,1,4,3}^{(4)f} + \mathcal{I}_{2,3,4,1}^{(4)f} \right), \\
M_{2,2}^{(4)} &= -\mathcal{I}_{1,2,3,4}^{(4)f2}.
\end{aligned} \tag{5.33}$$

The parentheses group the permutations of each integral. Note that here we use the scattering amplitude notation; corresponding conformal integrals follow simply from the graph duality illustrated in fig. 8.

We now equate the two representations (5.32) and (5.33). Since the integrals are evaluated off-shell ($x_{i,i+1}^2 \neq 0$) and are finite, we can use conformal symmetry and magic identities to relate the first five conformal integrals in fig. 14, with any order of their indexes, to a unique

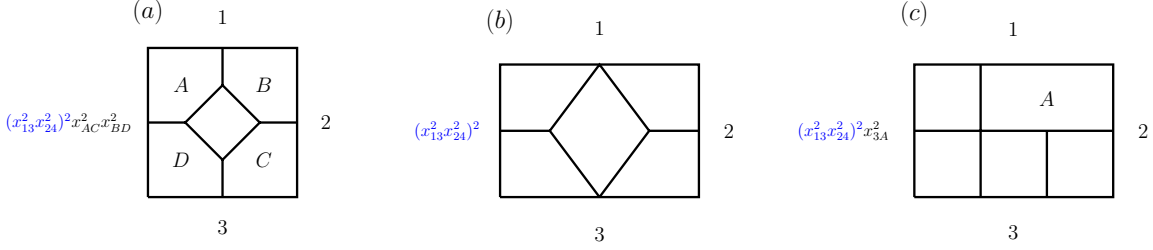


Figure 15: Five-loop conformal integrals contributing to the next-to-fishnet scattering amplitude $M_{2,2}^{(5)}$

This identity between regular fishnets Feynman diagrams and determinants of Ladders was first conjectured in [49] and later proven in [53, 54]. For us, this identity appears as a by-product of the relations (4.9) and (5.4) between the coulomb branch amplitude and octagons.

The first sub-leading loop order maps to a single determinant according to (5.31):

$$\begin{aligned}
 M_{n+l,n}^{[n(n+l)+1]} &= (-1)^{n+l-1} I_{n,l}^{[n(n+l)+1]} \\
 &= (-1)^{(n+1)(l+1)} 2(2n-1+l) F_{1+l, 3+l, \dots, 2n-1+l+1}.
 \end{aligned}
 \tag{5.39}$$

The left-hand side is now composed of various conformal integrals. The first instance of these partial amplitudes appears at five loops with $n = 2$, $l = 0$. It is given by the three integrals represented in fig. 15 and its permutations:

$$\begin{aligned}
 M_{2,2}^{(5)} &= -\mathcal{I}_{1,2,3,4}^{(5)a} + \left(\mathcal{I}_{1,2,3,4}^{(5)b} + \mathcal{I}_{2,1,4,3}^{(5)b} \right) - 2 \left(\mathcal{I}_{1,2,3,4}^{(5)c} + \mathcal{I}_{2,3,4,1}^{(5)c} + \mathcal{I}_{3,4,1,2}^{(5)c} + \mathcal{I}_{4,1,2,3}^{(5)c} \right) \\
 &= -6 F_{1,4} = -6 F_1 F_4 + F_2 F_3.
 \end{aligned}
 \tag{5.40}$$

In order to satisfy the dihedral symmetry the maximum number of permutations is 8, but this is lower when the graph has an extra symmetry. For instance the symmetric graph $\mathcal{I}^{(5)a}$ appears only once, the graph $\mathcal{I}^{(5)b}$ has two inequivalent permutations and the graph $\mathcal{I}^{(5)c}$ has no symmetry so it comes with the maximum number of permutations. After using conformal symmetry these eight graphs reduces to four with an overall factor of 2.

These integrals are unknown for generic values of the cross ratios, but they were computed at leading order in the OPE limit in [5] and we have checked those results are consistent with the prediction on the second line of (5.40).

At higher loops the number of distinct conformal integrals grows as can be seen in the data extracted from [3] for:

$$\{M_{2,3}^{(7)}, M_{2,4}^{(9)}, M_{3,3}^{(10)}\}.
 \tag{5.41}$$

Nevertheless, we were able to identify a simple pattern to construct the correspondent integrands. We conjecture that each integral in $M_{n+l,n}^{[n(n+l)+1]}$ can be obtained from the $(n+l) \times n$ regular fishnet of (5.38) by deforming one of its 2×2 sub-lattices in one of the three ways at the top of fig. 15 (including the numerators). After generating all integrals, we group them

into three families according to which deformation we used and add them up with overall coefficients $\{-1, +1, -1\}$ where the plus sign corresponds to the large diamond deformation (b). This linear combination gives the integrand of $M_{n+l,n}^{[n(n+l)+1]}$, as it happens in (5.40).

6 Discussion

In this paper we showed that a ten-dimensional symmetry unites the correlation functions of half-BPS scalar operators in four-dimensional $\mathcal{N}=4$ super-Yang-Mills theory with various R-charge. This symmetry is realized in a generating function for loop integrands, which depends exclusively on the 10D sum of spacetime and R-charge space distances (see eq. (3.21)). The symmetry is broken upon integration and does not simply follow from the 10-dimensional Lagrangian which underlies this theory. At least up to seven loops, it enables to compute all R-charge correlators from just the simplest case of stress-tensor correlators, and was confirmed using existing five-loop results in the literature.

One of the main consequences of this enlarged symmetry is an extension of the correlator/amplitude duality. This was obtained by equating two interpretations of the 10D null limit of the generating function: as a large R-charge limit giving the so-called octagon of section 5.2, or a scattering amplitude of massive W bosons on the Coulomb branch of the theory. Since these massive amplitudes are infrared-finite, this equality between correlators and amplitudes holds not only for the integrand but also at the integrated level. The duality currently only accesses a strict subset of the kinematic space of each object, which hints at a possible generalization of the correlation functions which would contain both as depicted in fig. 16.

Recent integrability-based results make it possible to write the octagon/amplitude as an infinite sum of well-studied determinants of infinite size (see eq. (5.8)). It is unclear whether the sum could be recast as a single infinite determinant. If possible, this would give, for the first time, a practical finite-coupling representation for a scattering amplitude in a 4D gauge theory.

The massless limit of the amplitude on the restricted Coulomb branch is curiously controlled by an exponent Γ_{oct} which differs from the cusp anomalous dimension Γ_{cusp} , as discussed in section 4.2. Recently these two anomalous dimensions were found to be governed by the same modified BES equation evaluated at two different values of the deformation parameter [55]. In light of this development, it is tempting to speculate that this parameter could be associated to different approaches to the massless limit.

Agreement between the octagon integrand and integrability results at weak coupling is nontrivial and predicts new analytic formulas for certain (sums of) integrals as determinants of ladder integrals (for example, eq. (5.35)). These relations extend the family of regular fishnets to a family of simple linear combinations of deformed fishnets, which also map to single determinants.

Our results are not unrelated to the ten-dimensional symmetry found in supergravity approximation in ref. [17]. The objects which satisfy the symmetry are precisely the same: in

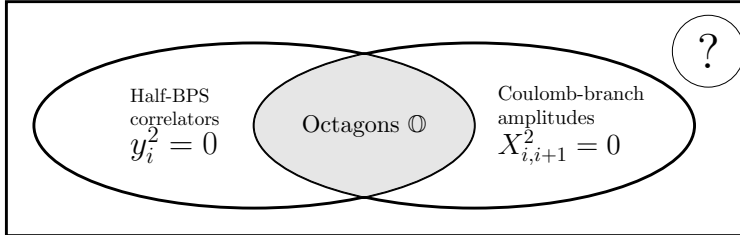


Figure 16: Half-BPS correlators are labelled by 10D coordinates (x, y) where y is a null 6D vector, while Coulomb branch scattering amplitudes are labelled by null-separated 10D points. These intersect on the restricted Coulomb branch, on which the octagons are defined. We can speculate on the existence of generalized correlators which satisfy a full 10D symmetry without any null condition.

both cases, the fields $\mathcal{O}(x)$ are packaged into “pre-ten-dimensional” ones $\mathcal{O}(x, y)$ by summing all R-charges according to eq. (3.1) and (2.1), and the symmetry is then only satisfied by the supersymmetrically *reduced* correlator \mathcal{H} (see eq. (3.21)).

While they apply to the same object, the two ten-dimensional symmetries are currently not connected: one holds in the weak coupling limit $g_{\text{YM}}^2 N_c \rightarrow 0$ while the other holds in the supergravity limit $g_{\text{YM}}^2 N_c \rightarrow \infty$. In between, the symmetry is not present: integration breaks the integrand-level symmetry at weak coupling, while stringy corrections to supergravity are also known to break related spectral degeneracies [56]. From the perspective of the present paper, it is hard to understand why the symmetry is restored in the infinite-coupling limit.

What could be the elusive operators in fig. 16, which measure $\mathcal{O}(x, y)$ when $y^2 \neq 0$? It is tempting to speculate that these could be related to D -instantons or D_{-1} -branes in the $\text{AdS}_5 \times S_5$ geometry. These already appeared in null-separated configurations in [20, 21]. To be more precise, the integrands, rather than just a representation of perturbation theory, are best viewed as exact $(n + \ell)$ -point correlators in self-dual Yang-Mills theory [25, 26]. We may thus speculate that the 10-dimensional integrands computed in the present paper are D_{-1} amplitudes in a putative bulk dual of self-dual super Yang-Mills. Why such correlators enjoy an accidental ten-dimensional conformal symmetry would still require additional explanation.

Acknowledgments

Work of S. C.-H. is supported by the National Science and Engineering Council of Canada, the Canada Research Chair program, the Simons Collaboration on the Nonperturbative Bootstrap, and the Sloan Foundation. Work of F. C. is supported in parts by the Canada Research Chair program and the Sloan Foundation.

A Definition of 3-loop conformal integrals

Here we present the basis of 3-loop conformal integrals that appear in the planar four-point functions of scalar single-trace operators, see (3.35). These are the 3-loop ladder (L), the tennis court (T), the easy (E) and hard (H) integrals, and finally a product of 1-loop and 2-loop ladder integrals ($g \times h$) :

$$\begin{aligned}
L_{13;24} &= \frac{(x_{24}^2)^2}{(\pi^2)^3} \int \frac{d^4 x_5 d^4 x_6 d^4 x_7}{(x_{15}^2 x_{25}^2 x_{45}^2) x_{56}^2 (x_{26}^2 x_{46}^2) x_{67}^2 (x_{27}^2 x_{37}^2 x_{47}^2)} \stackrel{\text{off-shell}}{=} \frac{F_3(z, \bar{z})}{x_{13}^2 x_{24}^2} \\
T_{13;24} &= \frac{x_{24}^2}{(\pi^2)^3} \int \frac{d^4 x_5 d^4 x_6 d^4 x_7 x_{17}^2}{(x_{15}^2 x_{25}^2) (x_{16}^2 x_{46}^2) (x_{27}^2 x_{37}^2 x_{47}^2) x_{56}^2 x_{57}^2 x_{67}^2} \stackrel{\text{off-shell}}{=} \frac{F_3(z, \bar{z})}{x_{13}^2 x_{24}^2} \\
E_{12;34} &= \frac{x_{23}^2 x_{24}^2}{(\pi^2)^3} \int \frac{d^4 x_5 d^4 x_6 d^4 x_7 x_{16}^2}{(x_{15}^2 x_{25}^2 x_{35}^2) x_{56}^2 (x_{26}^2 x_{36}^2 x_{46}^2) x_{67}^2 (x_{17}^2 x_{27}^2 x_{47}^2)} \\
H_{12;34} &= \frac{x_{14}^2 x_{23}^2 x_{34}^2}{(\pi^2)^3} \int \frac{d^4 x_5 d^4 x_6 d^4 x_7 x_{57}^2}{(x_{15}^2 x_{25}^2 x_{35}^2 x_{45}^2) x_{56}^2 (x_{36}^2 x_{46}^2) x_{67}^2 (x_{17}^2 x_{27}^2 x_{37}^2 x_{47}^2)} \\
(g \times h)_{13;24} &= \frac{x_{13}^2 (x_{24}^2)^2}{(\pi^2)^3} \int \frac{d^4 x_5}{x_{15}^2 x_{25}^2 x_{35}^2 x_{45}^2} \int \frac{d^4 x_6 d^4 x_7}{(x_{16}^2 x_{26}^2 x_{46}^2) x_{67}^2 (x_{27}^2 x_{37}^2 x_{47}^2)} \stackrel{\text{off-shell}}{=} \frac{F_1(z, \bar{z}) F_2(z, \bar{z})}{x_{13}^2 x_{24}^2}
\end{aligned} \tag{A.1}$$

All these integrals are known analytically in terms of single-valued harmonic polylogarithms [57].

B A five-loop identity

Following the comparison between amplitude integrals and determinants of ladders in section 5.3, we find the five-loop identity:

$$\begin{aligned}
 6 F_{1,4} = & \mathcal{P}_{2a^\circ} \left(\begin{array}{c} \text{Graph 1} \\ p_{1,3} p_{1,5} p_{2,4^2} p_{3,6} p_{3,7} \end{array} \right) + \mathcal{P}_{2b^\circ} \left(\begin{array}{c} \text{Graph 2} \\ p_{1,3} p_{2,4^2} \end{array} \right) + \begin{array}{c} \text{Graph 3} \\ -p_{1,3} p_{2,4^2} p_{5,6} \end{array} + \begin{array}{c} \text{Graph 4} \\ -p_{1,3} p_{1,7} p_{2,4^2} p_{3,6} \end{array} + \begin{array}{c} \text{Graph 5} \\ p_{1,3} p_{1,8} p_{2,4^2} p_{3,9} p_{5,6} \end{array} \\
 & \mathcal{P}_{4^\circ} \left(\begin{array}{c} \text{Graph 6} \\ -p_{1,3} p_{2,4^2} p_{3,8} \end{array} \right) + \begin{array}{c} \text{Graph 7} \\ -p_{1,3} p_{2,4^2} p_{3,7} \end{array} + \begin{array}{c} \text{Graph 8} \\ -p_{1,3} p_{2,4^2} p_{2,5} \end{array} + \begin{array}{c} \text{Graph 9} \\ -p_{1,3} p_{1,5} p_{2,4^2} \end{array} + \\
 & \begin{array}{c} \text{Graph 10} \\ -p_{1,3} p_{2,4^2} p_{3,5} p_{4,6} \end{array} + \begin{array}{c} \text{Graph 11} \\ p_{1,3} p_{1,8} p_{2,4^2} p_{2,6} p_{4,5} \end{array} + \begin{array}{c} \text{Graph 12} \\ p_{1,3} p_{1,5} p_{2,4^2} p_{2,7} p_{3,6} \end{array} + \begin{array}{c} \text{Graph 13} \\ p_{1,3} p_{1,7} p_{2,4^2} p_{2,5} p_{3,5} \end{array} + \begin{array}{c} \text{Graph 14} \\ p_{1,3} p_{1,5^2} p_{2,4^2} p_{3,6} \end{array}
 \end{aligned}
 \tag{B.1}$$

The numerators of the integrand are recorded below each graph, where $p_{a,b} \equiv x_{ab}^2$. The correspondent correlation-function graphs are found using graph duality as in fig. 8. We use the two-fold and four-fold permutation operators: $\mathcal{P}_{2a} X \equiv X + (1 \leftrightarrow 3)$, $\mathcal{P}_{2b} X \equiv X + (2 \leftrightarrow 4)$, and $\mathcal{P}_4 \equiv \mathcal{P}_{2a} \mathcal{P}_{2b}$.

References

- [1] B. Eden, P. Heslop, G. P. Korchemsky and E. Sokatchev, “Hidden symmetry of four-point correlation functions and amplitudes in $N=4$ SYM,” Nucl. Phys. B **862**, 193-231 (2012) [arXiv:1108.3557 [hep-th]].
- [2] B. Eden, P. Heslop, G. P. Korchemsky and E. Sokatchev, “Constructing the correlation function of four stress-tensor multiplets and the four-particle amplitude in $N=4$ SYM,” Nucl. Phys. B **862**, 450-503 (2012) [arXiv:1201.5329 [hep-th]].
- [3] J. L. Bourjaily, P. Heslop and V. V. Tran, “Amplitudes and Correlators to Ten Loops Using Simple, Graphical Bootstraps,” JHEP **11**, 125 (2016) [arXiv:1609.00007 [hep-th]].
- [4] D. Chicherin, J. Drummond, P. Heslop and E. Sokatchev, “All three-loop four-point correlators of half-BPS operators in planar $\mathcal{N} = 4$ SYM,” JHEP **08**, 053 (2016) [arXiv:1512.02926 [hep-th]].
- [5] D. Chicherin, A. Georgoudis, V. Gonçalves and R. Pereira, “All five-loop planar four-point functions of half-BPS operators in $\mathcal{N} = 4$ SYM,” JHEP **11**, 069 (2018) [arXiv:1809.00551 [hep-th]].
- [6] F. Coronado, “Perturbative four-point functions in planar $\mathcal{N} = 4$ SYM from hexagonalization,” JHEP **01**, 056 (2019) [arXiv:1811.00467 [hep-th]].
- [7] F. Coronado, “Bootstrapping the Simplest Correlator in Planar $\mathcal{N} = 4$ Supersymmetric Yang-Mills Theory to All Loops,” Phys. Rev. Lett. **124**, no.17, 171601 (2020) [arXiv:1811.03282 [hep-th]].
- [8] I. Kostov, V. B. Petkova and D. Serban, “Determinant Formula for the Octagon Form Factor in $N=4$ Supersymmetric Yang-Mills Theory,” Phys. Rev. Lett. **122**, no.23, 231601 (2019) [arXiv:1903.05038 [hep-th]].
- [9] I. Kostov, V. B. Petkova and D. Serban, “The Octagon as a Determinant,” JHEP **11**, 178 (2019) [arXiv:1905.11467 [hep-th]].
- [10] K. A. Intriligator, “Bonus symmetries of $N=4$ superYang-Mills correlation functions via AdS duality,” Nucl. Phys. B **551**, 575-600 (1999) [arXiv:hep-th/9811047 [hep-th]].
- [11] B. Eden, A. C. Petkou, C. Schubert and E. Sokatchev, “Partial nonrenormalization of the stress tensor four point function in $N=4$ SYM and AdS / CFT,” Nucl. Phys. B **607**, 191-212 (2001) [arXiv:hep-th/0009106 [hep-th]].
- [12] J. L. Bourjaily, A. DiRe, A. Shaikh, M. Spradlin and A. Volovich, “The Soft-Collinear Bootstrap: $N=4$ Yang-Mills Amplitudes at Six and Seven Loops,” JHEP **03**, 032 (2012) [arXiv:1112.6432 [hep-th]].
- [13] J. L. Bourjaily, P. Heslop and V. V. Tran, “Perturbation Theory at Eight Loops: Novel Structures and the Breakdown of Manifest Conformality in $N=4$ Supersymmetric Yang-Mills Theory,” Phys. Rev. Lett. **116**, no.19, 191602 (2016) [arXiv:1512.07912 [hep-th]].
- [14] S. Lee, S. Minwalla, M. Rangamani and N. Seiberg, “Three point functions of chiral operators in $D = 4$, $N=4$ SYM at large N ,” Adv. Theor. Math. Phys. **2**, 697-718 (1998) [arXiv:hep-th/9806074 [hep-th]].
- [15] F. Aprile, J. Drummond, P. Heslop and H. Paul, “Double-trace spectrum of $N = 4$

- supersymmetric Yang-Mills theory at strong coupling,” *Phys. Rev. D* **98**, no.12, 126008 (2018) [arXiv:1802.06889 [hep-th]].
- [16] F. Aprile, J. M. Drummond, P. Heslop, H. Paul, F. Sanfilippo, M. Santagata and A. Stewart, “Single particle operators and their correlators in free $\mathcal{N} = 4$ SYM,” *JHEP* **11**, 072 (2020) [arXiv:2007.09395 [hep-th]].
- [17] S. Caron-Huot and A. K. Trinh, “All tree-level correlators in $\text{AdS}_5 \times \text{S}_5$ supergravity: hidden ten-dimensional conformal symmetry,” *JHEP* **01**, 196 (2019) [arXiv:1809.09173 [hep-th]].
- [18] T. Fleury and S. Komatsu, “Hexagonalization of Correlation Functions,” *JHEP* **01**, 130 (2017) [arXiv:1611.05577 [hep-th]].
- [19] L. F. Alday, B. Eden, G. P. Korchemsky, J. Maldacena and E. Sokatchev, “From correlation functions to Wilson loops,” *JHEP* **09**, 123 (2011) [arXiv:1007.3243 [hep-th]].
- [20] L. F. Alday and J. M. Maldacena, “Gluon scattering amplitudes at strong coupling,” *JHEP* **06**, 064 (2007) [arXiv:0705.0303 [hep-th]].
- [21] N. Berkovits and J. Maldacena, “Fermionic T-Duality, Dual Superconformal Symmetry, and the Amplitude/Wilson Loop Connection,” *JHEP* **09**, 062 (2008) [arXiv:0807.3196 [hep-th]].
- [22] N. Beisert, R. Ricci, A. A. Tseytlin and M. Wolf, “Dual Superconformal Symmetry from $\text{AdS}(5) \times \text{S}^5$ Superstring Integrability,” *Phys. Rev. D* **78**, 126004 (2008) [arXiv:0807.3228 [hep-th]].
- [23] Z. Bern, L. J. Dixon, D. A. Kosower, R. Roiban, M. Spradlin, C. Vergu and A. Volovich, “The Two-Loop Six-Gluon MHV Amplitude in Maximally Supersymmetric Yang-Mills Theory,” *Phys. Rev. D* **78**, 045007 (2008) doi:10.1103/PhysRevD.78.045007 [arXiv:0803.1465 [hep-th]].
- [24] J. M. Drummond, J. Henn, G. P. Korchemsky and E. Sokatchev, “Hexagon Wilson loop = six-gluon MHV amplitude,” *Nucl. Phys. B* **815**, 142-173 (2009) [arXiv:0803.1466 [hep-th]].
- [25] L. J. Mason and D. Skinner, “The Complete Planar S-matrix of $\text{N}=4$ SYM as a Wilson Loop in Twistor Space,” *JHEP* **12**, 018 (2010) [arXiv:1009.2225 [hep-th]].
- [26] S. Caron-Huot, “Notes on the scattering amplitude / Wilson loop duality,” *JHEP* **07**, 058 (2011) [arXiv:1010.1167 [hep-th]].
- [27] B. Eden, G. P. Korchemsky and E. Sokatchev, “From correlation functions to scattering amplitudes,” *JHEP* **12**, 002 (2011) [arXiv:1007.3246 [hep-th]].
- [28] L. F. Alday, J. M. Henn, J. Plefka and T. Schuster, “Scattering into the fifth dimension of $\text{N}=4$ super Yang-Mills,” *JHEP* **01**, 077 (2010) [arXiv:0908.0684 [hep-th]].
- [29] S. Caron-Huot and D. O’Connell, “Spinor Helicity and Dual Conformal Symmetry in Ten Dimensions,” *JHEP* **08**, 014 (2011) [arXiv:1010.5487 [hep-th]].
- [30] Z. Bern, J. S. Rozowsky and B. Yan, “Two loop four gluon amplitudes in $\text{N}=4$ superYang-Mills,” *Phys. Lett. B* **401**, 273-282 (1997) [arXiv:hep-ph/9702424 [hep-ph]].
- [31] J. M. Drummond, J. Henn, V. A. Smirnov and E. Sokatchev, “Magic identities for conformal four-point integrals,” *JHEP* **01**, 064 (2007) [arXiv:hep-th/0607160 [hep-th]].
- [32] B. Eden, G. P. Korchemsky and E. Sokatchev, “More on the duality correlators/amplitudes,” *Phys. Lett. B* **709**, 247-253 (2012) [arXiv:1009.2488 [hep-th]].

- [33] Z. Bern, L. J. Dixon and V. A. Smirnov, “Iteration of planar amplitudes in maximally supersymmetric Yang-Mills theory at three loops and beyond,” *Phys. Rev. D* **72**, 085001 (2005) [arXiv:hep-th/0505205 [hep-th]].
- [34] A. V. Belitsky and G. P. Korchemsky, “Exact null octagon,” *JHEP* **05**, 070 (2020) [arXiv:1907.13131 [hep-th]].
- [35] T. Bargheer, F. Coronado and P. Vieira, “Octagons I: Combinatorics and Non-Planar Resummations,” *JHEP* **08**, 162 (2019) [arXiv:1904.00965 [hep-th]].
- [36] T. Bargheer, F. Coronado and P. Vieira, “Octagons II: Strong Coupling,” [arXiv:1909.04077 [hep-th]].
- [37] A. V. Belitsky and G. P. Korchemsky, “Octagon at finite coupling,” *JHEP* **07**, 219 (2020) [arXiv:2003.01121 [hep-th]].
- [38] A. V. Belitsky and G. P. Korchemsky, “Crossing bridges with strong Szego limit theorem,” [arXiv:2006.01831 [hep-th]].
- [39] A. V. Belitsky, “Null octagon from Deift-Zhou steepest descent,” [arXiv:2012.10446 [hep-th]].
- [40] I. Kostov and V. B. Petkova, “Octagon with finite bridge: free fermions and determinant identities,” [arXiv:2102.05000 [hep-th]].
- [41] B. Eden and A. Sfondrini, “Tessellating cushions: four-point functions in $\mathcal{N} = 4$ SYM,” *JHEP* **10**, 098 (2017) [arXiv:1611.05436 [hep-th]].
- [42] B. Basso, S. Komatsu and P. Vieira, “Structure Constants and Integrable Bootstrap in Planar $\mathcal{N}=4$ SYM Theory,” [arXiv:1505.06745 [hep-th]].
- [43] Y. Jiang, S. Komatsu, I. Kostov and D. Serban, “Clustering and the Three-Point Function,” *J. Phys. A* **49**, no.45, 454003 (2016) [arXiv:1604.03575 [hep-th]].
- [44] B. Basso and D. L. Zhong, “Three-point functions at strong coupling in the BMN limit,” *JHEP* **04**, 076 (2020) [arXiv:1907.01534 [hep-th]].
- [45] T. Fleury and S. Komatsu, “Hexagonalization of Correlation Functions II: Two-Particle Contributions,” *JHEP* **02**, 177 (2018) [arXiv:1711.05327 [hep-th]].
- [46] M. De Leeuw, B. Eden, D. Le Plat, T. Meier and A. Sfondrini, “Multi-particle finite-volume effects for hexagon tessellations,” *JHEP* **09**, 039 (2020) [arXiv:1912.12231 [hep-th]].
- [47] T. Fleury and V. Goncalves, “Decagon at Two Loops,” *JHEP* **07**, 030 (2020) [arXiv:2004.10867 [hep-th]].
- [48] N. I. Usyukina and A. I. Davydychev, “Exact results for three and four point ladder diagrams with an arbitrary number of rungs,” *Phys. Lett. B* **305**, 136-143 (1993)
- [49] B. Basso and L. J. Dixon, “Gluing Ladder Feynman Diagrams into Fishnets,” *Phys. Rev. Lett.* **119**, no.7, 071601 (2017) [arXiv:1705.03545 [hep-th]].
- [50] B. Basso, L. J. Dixon, D. A. Kosower, A. Krajenbrink and D. l. Zhong, “Fishnet four-point integrals: integrable representations and thermodynamic limits,” [arXiv:2105.10514 [hep-th]].
- [51] Z. Bern, M. Czakon, L. J. Dixon, D. A. Kosower and V. A. Smirnov, “The Four-Loop Planar Amplitude and Cusp Anomalous Dimension in Maximally Supersymmetric Yang-Mills Theory,” *Phys. Rev. D* **75**, 085010 (2007) [arXiv:hep-th/0610248 [hep-th]].

- [52] B. Eden and V. A. Smirnov, “Evaluating four-loop conformal Feynman integrals by D-dimensional differential equations,” *JHEP* **10**, 115 (2016) [arXiv:1607.06427 [hep-th]].
- [53] S. Derkachov and E. Olivucci, “Exactly solvable magnet of conformal spins in four dimensions,” *Phys. Rev. Lett.* **125**, no.3, 031603 (2020) [arXiv:1912.07588 [hep-th]].
- [54] S. Derkachov and E. Olivucci, *JHEP* **02**, 146 (2021) doi:10.1007/JHEP02(2021)146 [arXiv:2007.15049 [hep-th]].
- [55] B. Basso, L. J. Dixon and G. Papathanasiou, “Origin of the Six-Gluon Amplitude in Planar $N = 4$ Supersymmetric Yang-Mills Theory,” *Phys. Rev. Lett.* **124**, no.16, 161603 (2020) [arXiv:2001.05460 [hep-th]].
- [56] F. Aprile, J. M. Drummond, H. Paul and M. Santagata, “The Virasoro-Shapiro amplitude in $\text{AdS}_5 \times \text{S}^5$ and level splitting of 10d conformal symmetry,” [arXiv:2012.12092 [hep-th]].
- [57] J. Drummond, C. Duhr, B. Eden, P. Heslop, J. Pennington and V. A. Smirnov, “Leading singularities and off-shell conformal integrals,” *JHEP* **08**, 133 (2013) [arXiv:1303.6909 [hep-th]].